Analysis of Energy Efficiency Strategies in Residential Buildings

Thesis

Presented in Partial Fulfillment of the Requirements for the Degree Master of Science
in the Graduate School of The Ohio State University

By

Kara Ashley Shell, B.S.M.E.

Graduate Program in Mechanical Engineering

The Ohio State University

2010

Thesis Committee:

Mark E. Walter, Advisor

Gary L. Kinzel

Abstract

In response to the fact that residential buildings consume a significant amount of the energy produced within the United States, students at The Ohio State University undertook to design and build two small, solar powered homes. These homes are now public demonstrations of the feasibility of energy-efficiency, solar energy, and sustainability in residential homes. The effectiveness of each of the houses major components are discussed and evaluated using both analytical and numerical methods. Results show that significant energy savings can be achieved by employing solar power generation, solar hot water heating, energy-efficient building materials, gray water recycling, and passive solar heating. Passive solar heating using a thermal storage wall incorporating phase change material is evaluated in more detail to determine the effects of wall materials on performance. The thermal storage wall analysis indicates that the incorporation of phase change material (PCM) and the glazing material has a subtantial effect on the wall performance, but the PCM encapsulation material is less important. The study suggested several improvements to the original house thermal storage wall design.

Dedication

Dedicated to my parents for instilling in me the desire and drive to succeed.

Acknowledgements

I would like to acknowledge my project advisors, Dr. Mark Walter, Dr. Gary Kinzel, and Dr. Seppo Korpela, without whom none of this work would be possible. I would also like to recognize my family and friends, who supported me without fail as I pursued my graduate degree. I sincerely thank you all.

Vita

May 2004……………………………………………Hilliard Darby High School

December 2008…………………………………..B.S. Mechanical Engineering

January 2008 to present…………………………Graduate Research Assistant,
Department of Mechanical Engineering,
The Ohio State University

Fields of Study

Major Field: Mechanical Engineering

Table of Contents

List of Tables

List of Figures

Introduction

In response to the large energy consumption of residential buildings in the United States, students at The Ohio State University undertook to design and build two small, solar powered homes. These homes are now demonstrations to the public of the feasibility of energy efficiency, solar energy and sustainability in the residential buildings sector. Chapter 1 discusses the solar strategies employed in a small, sustainable home to be displayed at the Center of Science and Industry in Columbus, Ohio. Solar power generation, solar hot water heating, and passive solar heating using a phase change material (PCM) for heat storage are discussed. The annual energy and financial savings for each system are calculated, to illustrate the payback period and feasibility of investment in the described technologies. Chapter 2 assesses in more detail passive solar heating using phase change material. The design of the thermal storage wall incorporated in the 2009 Ohio State University Solar Decathlon house is evaluated using finite element analysis in FLUENT for representative mild, moderate and severe winter days. The effects of the container and glazing material are discussed. Finally, a comparison of the wall performance with and without PCM is performed. Both analyses illustrate the performance and feasibility of energy efficiency strategies in residential homes.

Chapter 1:

The Design and Construction of a Small House as an Exhibit and Test Platform for Sustainability and Reduced Energy Consumption

Abstract

In response to the significant energy consumption of the residential-building industry, an interdisciplinary team of architecture and engineering students designed and built a small home as a test platform for sustainable technologies. The goal of the project was to integrate engineering energy-saving strategies into the home in an interesting way, and display the home to the public as an exhibit. At the same time, the performance of the systems will be monitored to determine success and suggest modifications. The home achieves significant energy savings by employing solar power generation, solar hot water heating, energy efficient building materials, phase change material, and gray water recycling. The home successfully supports available and emerging sustainable technologies, and will generate homeowner awareness when installed as an exhibit at the Center of Science and Industry in Columbus, Ohio.

1. Introduction

The depletion of non-renewable fuels, global climate change, and awareness of the impact of harmful emissions on health and the environment has led to an increased interest in renewable energy and energy efficiency applied to every major energy sector. However, the most energy and environmental gains can be achieved by focusing efforts on improving the energy efficiency and building practices in residential and commercial buildings. Data collected by the Energy Information Administration shows that buildings account for 37% of the energy used in the United States, and of that energy, 53% is consumed by residential buildings [1].

Considering the large energy consumption of the residential-buildings sector, efforts to decrease energy use and negative environmental impact is an important national issue. There are two major obstacles to improving sustainability in residential buildings. One is the technology. The energy efficiency of appliances, lighting, HVAC, and building materials must continue to improve. And not only must the technology improve, but the cost must decrease to a point where it can compete economically with traditional building materials and practices. Two, homeowners and residential contractors are often unaware of the technology and materials available, or have negative impressions of the cost or ease of installation. Both of these concerns must be addressed for a positive impact in residential buildings to be achieved.

In 2007, an interdisciplinary team of three architecture and three mechanical engineering students at the Ohio State University initiated a project to design and build a small, sustainable home as a senior design project. By working together, the team incorporated the engineering technologies into the architectural design of the house from the very beginning. Furthermore, the house would be an exhibit of sustainable building and living strategies. As many sustainable technologies would be incorporated in the home as possible, covering a wide range of cost and complexity. Therefore anyone who toured the house would be able to learn about something they could do in their own home. In this way, the house would meet both of the needs for furthering sustainability in residential homes by supporting sustainable technologies and increasing public awareness. The project was so successful that it will become an exhibit at the Center for Science and Industry in Columbus (COSI). Approximately 0.5 million people visit the COSI facility each year.

2. Sustainable Technology

As many of the currently available sustainable technologies were incorporated into the house as possible, both to improve its overall energy efficiency and environmental impact and also to educate the public on their use. The engineering technologies were sized for 1-2 people engaged in an energy-conscious standard of living. The systems were also designed for off-grid installation. However, some adaptations to the house allow for it to be a successful exhibit and test platform. When installed at COSI, the house will be connected to the water, sewage, and electrical grids to provide water and sewage facilities as well as emergency backup power. These modifications are necessary for the intended performance and safety of the home as an exhibit. It is also intended for the house to be a test platform for these technologies. To this end, there is no backup heating or cooling included in the house design, and the backup hot water heating is optional. It is intended that the performance of the solar power generation system, solar hot water heating system, and passive solar heating of the building will be monitored. The results will determine the effectiveness of the technologies without assistance and what modifications should be made to the design. If it is necessary for the function of the exhibit, electric resistance heaters can be used to heat both the interior of the house and the hot water tank.

2.1 Solar Power Generation

The house includes an off-grid solar power system, where the solar array was sized to produce 100% of the energy required to run the home year-round. The system is called “off-grid” because it is not intended to be connected to the nation’s electrical grid. A diagram of the power system can be seen in Figure 1.1. The system consists of a quantity of photovoltaic modules that provide power to a battery charge controller. The charge controller regulates the voltage to safely charge a set of batteries. An inverter that simulates electrical grid quality power is connected to the batteries to provide alternating current power to the house.

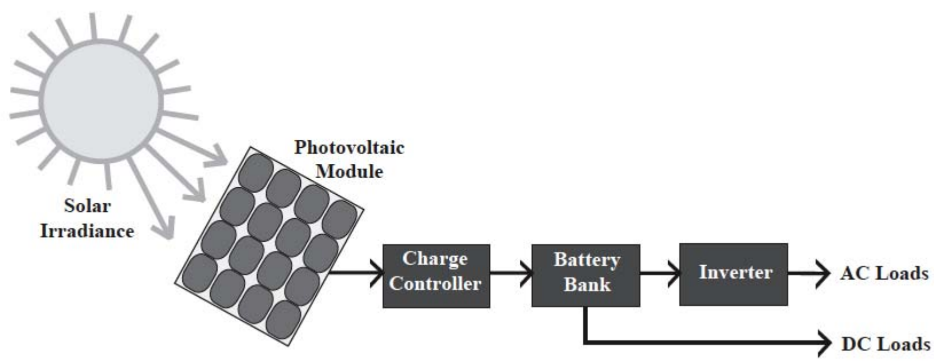

Figure 1.1: Photovoltaic System Diagram

The daily electrical requirements were estimated for the house in both summer and winter configurations. This estimate required the specification of all of the appliances that would be used in the house at an early stage in the project. The results of the electrical use estimation are shown in Table 11.

Table 1.1: Seasonal Electricity Use Estimation

Appliance	Power Consumption (Watts)	Usage per Day (hr)	Daily Power Consumption (Watt-hr)
SUMMER			
Refrigerator	36	24	864
Fans	32	8	256
Laptop Charging	60	4	240
Lights	30	4	120
Pump Station	72	2	144
Cell Phone Charging	8	4	32
Gray Water System	36	0.25	9
		Summer Total	**1665**
WINTER			
Lights	30	8	240
Laptop Charging	60	4	240
Pump Station	72	2	144
Refrigerator	36	2	72
Fans	32	2	64
Cell Phone Charging	8	4	32
Gray Water System	36	0.25	9
		Winter Total	**801**

The size of the solar array required was then calculated using the electrical use estimations as well as daily solar irradiance data for Columbus, Ohio. Sun hours per day in the units of $kWh/(m^2 \ day)$ are cataloged for major US cities. The average daily value of sun hours in Columbus is 5.26 in the summertime and 2.66 in the wintertime [3]. The size of the solar array required for a given load and level of sun hours can be calculated with Eq (1.1). The calculations show the minimum size for the installation is 316.5W.

Load (Wh/day) = Array Size (W) × Sun Hours (hr/day) (1.1)

$$\text{Summer:}\ \ 1665\ W \cdot h = x \cdot 5.25\ {}^{h}\!/_{day} \Rightarrow x = 316.5\ W$$

$$\text{Winter:}\ \ 801\ W \cdot h = x \cdot 2.66\ {}^{h}\!/_{day} \Rightarrow x = 301.1\ W$$

The solar panels chosen have a power output of 12W with a voltage rating of 12V each. The charge controller required 48 V, which is accomplished by wiring 4 panels together in series, and then combining each set of 4 panels in parallel before connecting to the charge controller. This meant that the number of panels used must result in an array output greater than 316.5 W, and also be a multiple of 4. The final array consisted of 32 solar panels with a total rated output of 386 Watts.

Batteries were employed to provide electricity to the house during off-peak hours. The group specified that the house should be able to operate for 5 days from a complete charge with no incident solar radiation. This value was selected based on guidelines for off-grid living and to allow the batteries to stay well above the 50% charged level during normal operation. The maximum power required by the house is the summer value of 1665 Wh, for an estimated possible maximum of 4 days without significant sunlight. The required battery size was determined using Eq (1.2). From the calculation, an array of six 100 Ah batteries were selected.

$$\text{Load}\left(\mathrm{W \cdot h}\!/_{\mathrm{day}}\right) \times \frac{1\ \mathrm{A}}{12\ \mathrm{W}} \times \text{Time (days)} = \text{Battery Size } (\mathrm{A \cdot h})\ \mathit{Load} \qquad (1.2)$$

$$1665\, {}^{W \cdot h}\!/_{day} \times \frac{1A}{12W} \times 4 days = 555 A \cdot h$$

Other necessary components for the solar-power system included a modified sine wave inverter to create alternating current, battery charge controllers, wiring, disconnect switches, and breakers. These components were specified to comply with standard photovoltaic installation practices and local electrical codes.

The cost of the system installation is summarized in Table 1.2 below. The payback period for the installation could be determined by extrapolating the electricity price and calculating the accumulated savings each year. The yearly output of the array was calculated to by 380 kW-h per year using the PV Watts Version 1 Solar Calculator [4]. The historical and extrapolated residential-electricity price as a function of time is shown in Figure 1.2 [5], and the accumulated savings each year are compared to the system cost in Figure 1.3. The estimated payback period for the house solar system is 37 years. The long payback period is a result of the very high energy efficiency of the house and the low cost of energy in Ohio. The house was designed to use as little energy as possible, so that equivalent annual cost savings would be small. This is common with very high-efficiency homes. However, an inherent benefit is that the system is 100% off-grid, making the design very valuable in a location where electricity is not readily available.

Table 1.2: Photovoltaic System Costs Summary

PHOTOVOLTAIC SYSTEM COSTS	
Item Description	**Cost, U.S. Dollars**
12W Photovoltaic Panels (32)	4800
Inverter, Charge Controller, Fuses, Wire, etc	835
Batteries	600
Miscellaneous Electrical	120
Total	**6355**

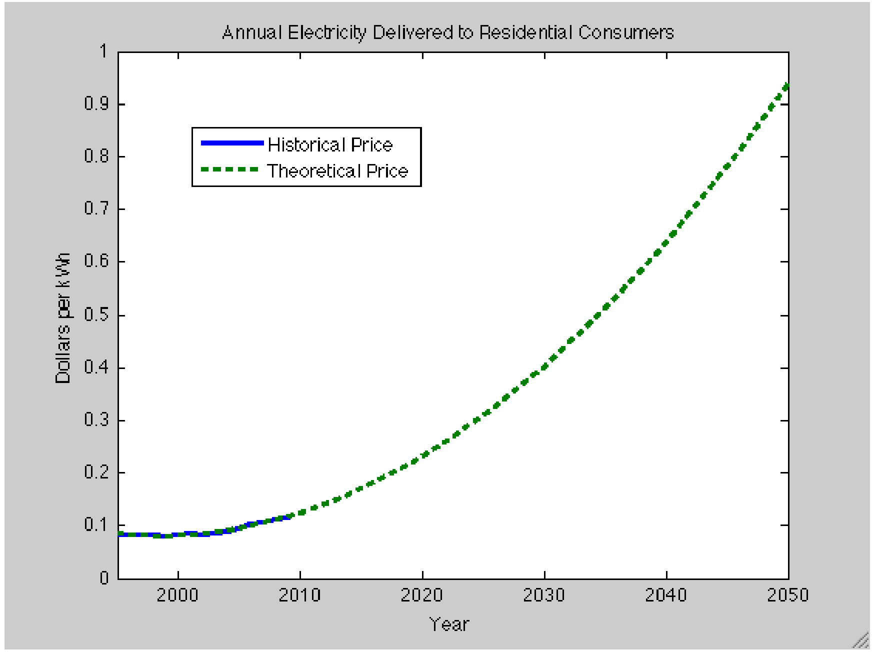

Figure 1.2: Historical and Theoretical Future Electricity Price

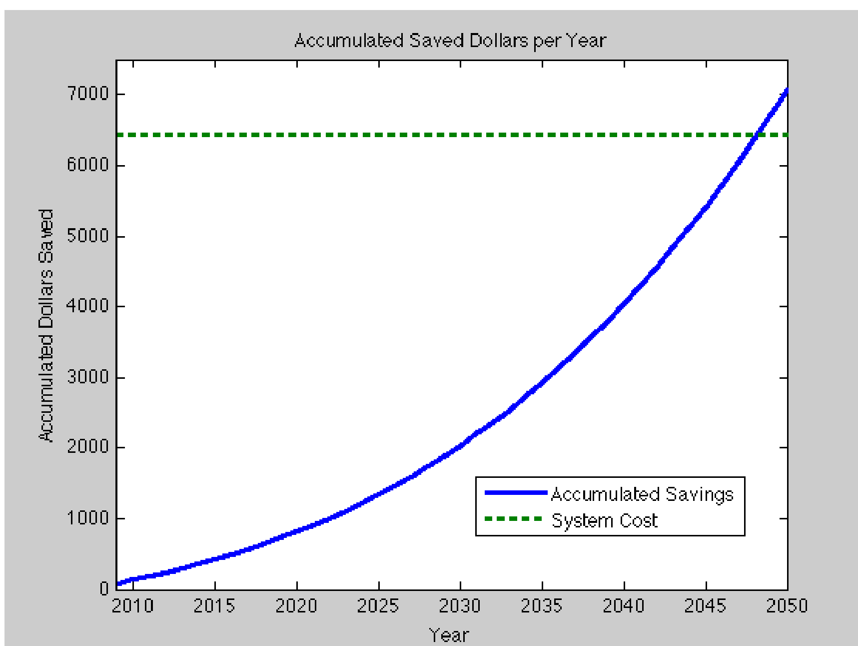

Figure 1.3: Accumulated Saved Dollars per Year

2.2 Solar Hot Water Heating

A solar hot water heating system was used to supply the residence with hot water. A schematic of the system can be seen in Figure 1.4 below. Solar radiation is absorbed by the collector and heats a glycol-water antifreeze mixture that is pumped through the collector. The antifreeze mixture is necessary to prevent the water in the collector from freezing. The heated antifreeze solution travels to a heat exchanger that transfers energy between the antifreeze solution and the potable water used in the home. A traditional natural gas hot water tank is used to store the potable hot water and supply auxiliary heat when necessary.

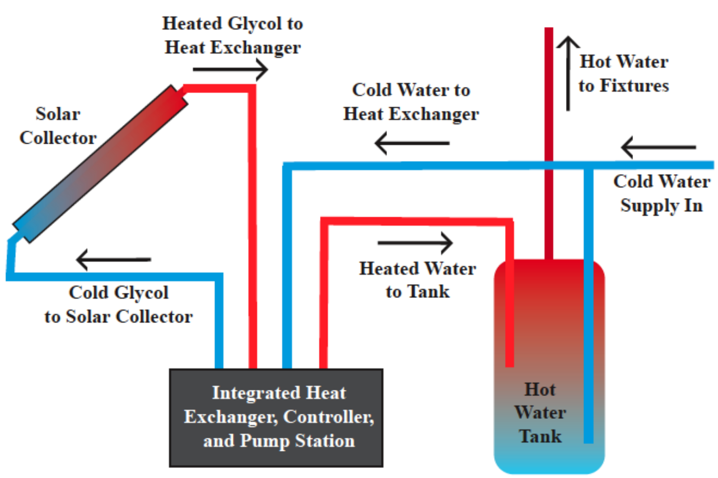

Figure 1.4: Solar Hot Water Heating System

The specifications for the solar hot water heating system were calculated by again estimating the daily energy demands of the residents of the house. Table 1.3 below shows the estimated hot water usage of two residents. The amount of energy required using the total daily hot water usage could then be calculated using Eq (1.3) [6].

Table 1.3: Hot Water Use Estimate for Two Residents

HOT WATER		
Time	**Volume, L**	**Use**
7:00 AM	7.6	Wash Hands and Face
1:00 PM	9.5	Wash Hands and Food Preparation
5:00 PM	12.1	Wash Hands and Laundry / Food Preparation
9:00 PM	56.8	Shower
11:00 PM	2.0	Wash Hands
Total	**88.0**	

$$Q_{used} = V \cdot \rho \cdot c_p \cdot (T_{used} - T_{in}) \tag{1.3}$$

Where:

Q_{used} = energy used in kJ/day
V = volume of water used = 88.0 L
ρ = density of water = 1.00 kg/m^3
c_p = specific heat of water = 4.186 kJ/kg-C
T_{used} = 48.9 °C (120 °F)
T_{in} = 12.8 °C (55 °F)

$$Q_{used} = 88.0 \, {}^{L}\!/_{day} \times 1.00 \, {}^{kg}\!/_{m^3} \times 4.186 \, {}^{kJ}\!/_{kg \cdot C} \times (48.9 - 12.8)°C = 13,298 \, {}^{kJ}\!/_{day}$$

The amount of heat lost through the hot water tank was then calculated with the R-value and surface area of the tank. This calculation was done with Eq (1.4).

$$Q_{lost} = \frac{1}{R} \cdot SA \cdot (T_{used} - T_a) \cdot h \tag{1.4}$$

Where:

Q_{lost} = amount of heat lost to the environment through the tank in kJ/day
R = R-value of the tank insulation = 0.3913 $m^2 \cdot h \cdot °C/kJ$
SA = surface area of the tank = 2.0 m^2
T_{use} = 49.0 °C (120 °F)
T_a = 15.6 °C (60 °F)
h = 24 h/day

$$Q_{lost} = \frac{1}{0.3913\, m^2 \cdot h \cdot °C / kJ} \times 2.0 m^2 \times (49.0 - 15.6)°C \times 24\ h/day = 4{,}097\ kJ/day$$

The total energy needed was then calculated as 13,298 + 4.097 = 17,395 kJ/day. A solar thermal collector manufacturer, SolarHOT, was consulted for the selection of an appropriate collector that would minimize the amount of auxiliary heat used. A 2.97 m^2 high-efficiency collector was selected. Table 1.4 below shows the specifications for the selected panel [7]. This panel will provide all of the hot water needs of the house during the warm seasons and provide most of the hot water needs during the winter. A larger collector was not used to reduce the capitol expenditure of the system and maximize the allowable roof-space for solar photovoltaic panels.

Table 1.4: kJ Provided Per Day by Selected Flat Plate Solar Collector

	kJ Provided per Day by Solar Hot Water Collector		
Season	**Clear** (196.0 kJ/m^2-day)	**Mildly Cloudy** (147.0 kJ/m^2-day)	**Cloudy** (98.0 kJ/m^2-day)
Summer	32710	22150	12660
Winter	22150	12660	3165

An integrated heat exchanger water pump system was selected from the manufacturer. The unit monitors the temperature of the glycol from the collector controls the pumps for maximum system efficiency. The remaining balance of the system, such as piping, insulation, and expansion tanks were installed to follow industry best practices and local regulations.

The cost of the system installation is summarized in Table 1.5 below. Because the auxiliary heat source would be natural gas, the payback period for the installation could be determined by extrapolating the natural gas price and calculating the accumulated savings each year. Historical and extrapolated residential natural gas prices are shown in Figure 1.5 [8], and the accumulated savings each year are compared to the system cost in Figure 1.6. The estimated payback period for the solar hot water system is 19 years. The reason that the payback period is so long is that the house was designed to greatly conserve hot water – so very little hot water is estimated to be used. This means that the payback period is greater than it would be in a standard home installation.

Table 1.5: Solar Hot Water System Costs

SOLAR HOT WATER SYSTEM COSTS	
Item Description	**Cost, U.S. Dollars**
4'x8' Flat Plate Collector	1300
Integrated Controller and Pump Station	1670
Mounting Hardware	100
5 gal of glycol antifreeze solution	120
Hot Water Tank, Piping, Insulation, Valves	300
Total	**3490**

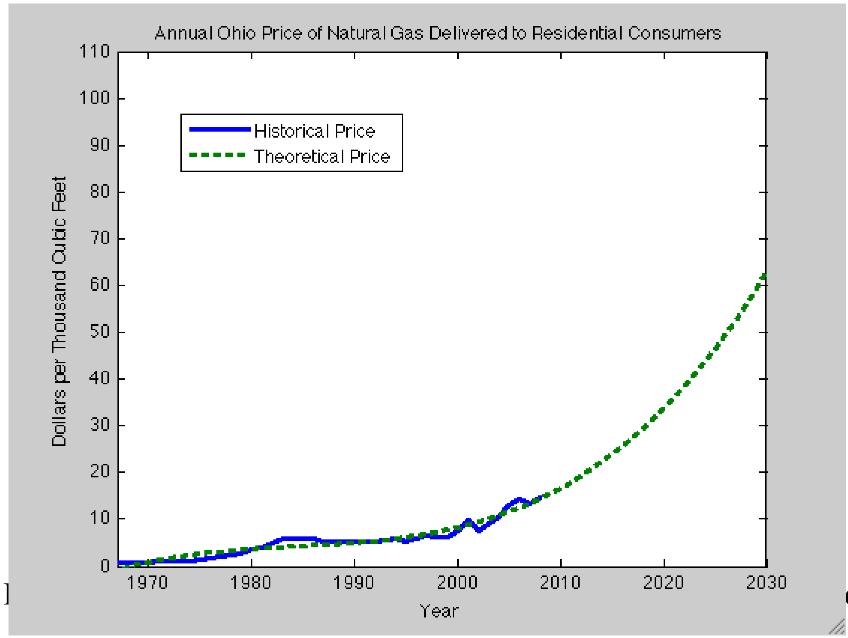

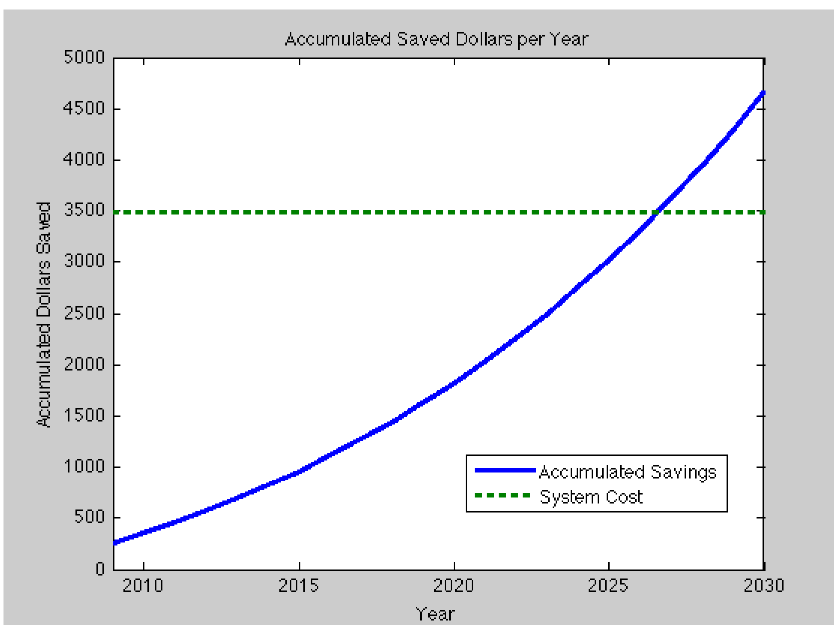

Figure 1.6: Accumulated Saved Dollars per Year

2.3 Passive Solar Heating and Cooling

Heating and cooling in the house is accomplished entirely passively, with no heating or cooling equipment. There are two keys to the success of this strategy. First, the home's design and construction must reduce the heat load as much possible. Utilizing high R-value insulation, minimizing air leaks, and using energy efficient doors and windows helps accomplish this. Secondly, phase change materials (PCMs) are used to mediate the energy absorbed by the house. PCMs absorb and retain thermal energy from the sun during the day and release it into the house at night. This reduces the peak heating and cooling loads in the home.

2.3.1 Structurally Insulated Panels

The house is constructed using Structurally Insulated Panels (SIPs), which are made of expanded polystyrene foam (EPS) foam sandwiched between two sheets of 1/2" oriented stand board (OSB). The thickness of the panel determines its insulation value – with typical foam thicknesses of 3.5", 5.5", 7.25", 9.25", and 11.25" (89 mm, 140 mm, 184 mm, 235 mm, and 286 mm) based on the standard American widths of lumber. There are several benefits to using SIPs for construction. Each SIP is constructed from airtight components, minimizing air leakage through the wall. The larger size of the SIPs panel means there are fewer thermal bridges in the wall caused by lumber cross-pieces. And the foam cores of SIPs are better insulation than fiberglass. This results in SIPs performing significantly better than standard wood frame construction. Table 1.6 compares the whole wall R-value of a 3.5" (89 mm) EPS core SIP to 2x4 and 2x6 (38x89 mm and 38x140 mm) wall construction with fiberglass batt insulation [9].

Table 1.6: Whole Wall R-value Comparison between 3.5" (89 mm) Core SIPs and Conventional 2x4 and 2x6 Wood Frame Walls

WALL CONSTRUCTION	WALL R-VALUE, m^2-h-C/kJ
SIP Normal	2.208
SIP Best Practice	2.233
2x4 @ 16" o.c. (38x89 mm @ .41 m o.c.)	1.518
2x4 @ 24" o.c. (38x89 mm @ .61 m o.c.)	1.555
2x6 @ 24" o.c. (38x140 mm @ .61 m o.c.)	2.170

Beyond the performance of the material itself, it has been found that construction using SIPs requires approximately half of the labor effort of standard wood frame construction [10]. This factor largely contributed to its selection as the construction material for the house.

2.3.2 Fenestration

The windows and doors were an important energy feature in the building design. Glass was used for both windows and doors, also called fenestration or glazing. Optimizing the location and quantity of fenestration surface area is important especially for passive heating. To heat a building passively in the winter, there must be a large amount of south facing glazing, and the glazing must have a high solar heat gain coefficient (SHGC) and low U-factor and emissivity. However, during the summer it is valuable to have a low SHGC, causing most energy-star rated windows to use low SHGC glass. The solar heat gain coefficient measures how well a product blocks heat from the sun. SHGC range from 0 to 1, with the ratio corresponding to the percentage of solar heat gain allowed [11]. U-factor measures the rate of heat transfer through a product. It is affected by conductivity of the glass, airflow around the window, and the emissivity of the glass. A lower U-factor value means that the product will better insulate the building. This is important in the winter to keep heat in and in the summer to keep heat out. Finally, emissivity is the ability of a product to absorb light energy and radiate it out into a room. Recently there have been significant technological advances in low-emissivity (low-e) coatings for glass, and this makes a valuable addition to the windows of a home [12]. The house uses energy star certified dual-pane, argon-blend glass with a low-e coating. The NFRC ratings for the windows give a SHGC of 0.27, meaning 27% of the sun's heat gain is transferred through the window. The window has a U-factor of 0.30. These values significantly impact the passive heating and cooling of the home.

2.3.3 Phase-Change Material (PCM)

The final strategy for mediating the heating and cooling loads of the house involved the integration of a phase-change material as a thermal storage device. Materials store energy as they are changing phase, and the temperature of the material remains constant while the thermal energy is used for the phase change. Then, when the temperature drops below the melting point, the energy stored is released. PCMs can be used to mediate cooling and heating loads by storing thermal energy during the day and releasing it at night. By using a PCM, overall heating and cooling loads are reduced, thereby decreasing the size of the required heating and cooling equipment and lowering the initial cost. PCM is also an effective way to delay the peak heating and cooling loads to times to off-peak electricity consumption hours. In places where electricity rates are based on peak or off-peak times, this can result in considerable savings [13].

There are several material properties that should be considered when selecting an appropriate PCM. Most important is the melting point of the material. It should be as close as possible to the desired interior temperature of the building. Another is the heat of fusion. The heat of fusion is the quantity of thermal energy required per unit mass of material to change phase. For PCM, the largest heat of fusion possible is desired, so that as much energy can be stored in a specific volume of PCM as possible. Another consideration is that most PCMs have a very low thermal conductivity. This significantly lowers the materials ability to "absorb" heat from the building, and also to release it. The safety of the material must also be considered. Numerous PCMs are unstable, volatile or flammable. Finally, the cost is an important factor. Many PCM materials are very expensive, and the initial cost outweighs the energy saving benefits.

Most PCMs can be classified as one of three types: Organics, Inorganics, and Eutectics. These can further be broken-down into various subcategories. Figure 1.7 shows the classes of PCM materials [14].

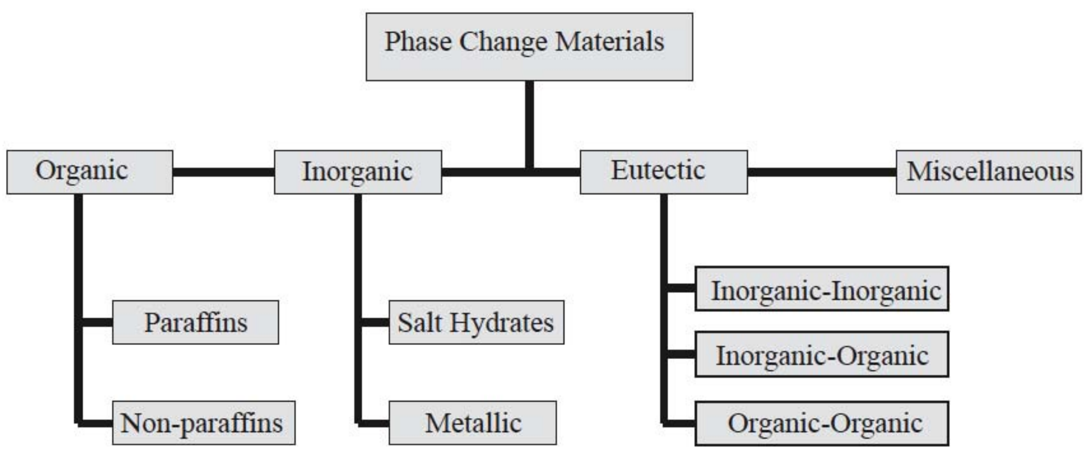

Figure 1.7: Classifications of PCM Materials

Each classification of PCM has its own advantages and disadvantages. Table 1.7 shows some material properties for PCMs with a melting point in the residential-comfort zone, between 20-24 °C. Organic paraffins are the most common commercially used PCM. They are waxy liquids or solids which are safe to handle and very stable. They have a very high heat of fusion, but a low thermal conductivity. They are also extremely flammable, which has caused them to be unfavorable for residential applications. Non-paraffins are the largest class of PCM materials. Their properties vary widely, depending on the material [15]. Hydrated salts are the most common inorganic PCM. They are attractive because they have high heats of fusion, high thermal conductivity, are non-flammable and inexpensive. However, they are generally corrosive and incompatible with many types of containers or building materials. They often experience phase segregation during transition and require the use nucleating and thickening agents, complicating their application. Eutectic materials are mixtures of two or more PCMs to achieve the desired melting point and material properties [14].

Table 1.7: Material Properties of PCMs with Appropriate Melting Point for Residential Applications [15]

Classifiation	Material	Melting Point, °C	Heat of Fusion, kJ/kg
Paraffin	n-Hexadecane	18.2	238
	n-Heptdecane	22	215
Non-paraffin	Lithium Chloride Ethanolate	21	188
	Polyethylene Glycol 600	20-25	146
	Butyl Stearate	19	140
	Dimethyl Sabacate	21	120-135
Salt Hydrate	NaCl.Na2SO410H2O	18	286
	KF.4H2O	18	330
	K2HO4.4H20	18.5	231
	Mn(NO3)2.6H2O	25	148
Eutectic	Na2SO4+NaCl+H2O	18	unavailable
	Na2S4+MgSO4+H2O	24	unavailable
	C14H28O2+C10H20O2	24	147.7

There are no PCMs with the perfect combination of melting point, heat of fusion, thermal conductivity, safety and cost. The best PCM is selected depending on the individual needs of the project. It was determined that the melting point and the safety were the most important attributes of the material. The interior temperature of the house would be a simple parameter to monitor and compare to the PCM melting point, easily allowing us to determine the effectiveness of the material. Safety was a key concern because the material would be in an exhibit on display in a child focused science center. So there must be no harmful properties of the material.

The material selected for thermal storage was polyethylene glycol (PEG) 600. This material has a melting point of 20-25°C (Particular melting point depends on the batch of the chemical). OSHA does not consider it a hazardous material, and it has NFPA ratings of 1 for Health, 1 for Fire, and 0 for Reactivity. Furthermore, PEG 600 is often used for pharmaceutical and personal care products. This information is evidence of the very safe nature of the material, making it suitable for this application [16]. The important properties of PEG 600 are summarized in [17].

The PCM was incorporated into the floor of the house, both for visibility and to maximize the solar heat storage of the material. To help aid thermal conduction, the PCM is contained in aluminum pans set within the floor. The aluminum pans come in varying sizes, and were used to form a gradient pattern on the floor. The larger size pans and greater quantity of PCM are located closer to the windows for maximum thermal storage, and the smaller pans are located further from the windows where shading will cause this area to be in the sunlight less often. The pans are covered with a clear Plexiglas pane, through which the public can see the material. Figure 1.8 shows the holes in the floor where the pans of PCM will be stored. A total of 79.5 liters of PCM are incorporated into the floor. This is another example of the integration of architectural design and engineering.

Figure 1.8: Picture of the Floor with Locations of Visible PCM storage

The performance of the construction materials and PCM could be evaluated by calculating the heating and cooling loads for the house. The heating and cooling loads were determined using the equations outlined in Chapter 17 of the ASHRAE Fundamentals Handbook [18]. Table 1.8 shows the house design conditions, Table 1.9 shows the house characteristics, and Table 1.10 shows the calculated envelope loads from each component and the total heating and cooling envelope load. It was found that the total heating load would be 2547 kJ/h and the total cooling load would be 4250 kJ/h.

Table 1.8: House Design Conditions

Item	Heating	Cooling	Notes
Latitude	-	-	39.99N
Elevation	-	-	249 m
Indoor Temperature	20.0 °C	23.9 °C	
Indoor RH	N/A	50%	no humidification
Outdoor Temperature	-12.8 °C	31.5 °C	99% heating, 1% cooling
Daily Range	N/A	8.8 °C	
Outdoor wet bulb	N/A	22.7 °C	MCWB @1%
wind speed	6.71 m/s	3.35 m/s	default assumption
Design Δt	32.8 °C	7.6 °C	

Table 1.9: House Characteristics

Component	Factors	Description
Roof/Ceiling	U=.0235, α=.3	Ch 17, Table 8
Exterior Walls	U=.0377	
Floor	U=.0214	
Windows	U=.30, SHGC=.27, T=.45	Vinyl-Clad Wood Frame, Dual-Pane Low-E Tempered Glazing with Argon, no interior shading
Construction	A_{ul}=.02	Well sealed construction

Table 1.10: Calculated Envelope Loads and Total Load

Component	Quantity (m^2)	Heating Load, kJ/h	Cooling Load, kJ/h
Ceiling	26.01	408.90	31.56
Wall	44.41	1119.85	214.39
Floor	21.27	-	129.62
S-Operable Window	1.10	221.67	872.55
S-Operable Window	1.10	221.67	872.55
S-Operable Window	1.10	221.67	872.55
SE-Operable Window	1.01	204.51	1053.87
N-Fixed Window	0.74	149.14	202.8
ENVELOPE TOTAL LOAD		**2547.39**	**4249.89**

The peak heating and cooling loads were used to calculate the amount of energy needed to heat and cool the house. This is accomplished using the classical bin method [19]. The bin method divides the U.S. into several climatic regions, and uses the average data for the particular region to calculate loads. For each climate region, the number of cooling (N_C) and heating (N_H) hours per year is given. The average temperatures for a given region are split into 2.78 °C "bins" which then have a fractional bin hours value, f, that identifies how many heating or cooling hours are spent in that temperature range. Columbus, Ohio is in climate region III. Climatic data and fractional bin hours for all of the climate regions can be found in [19].

To calculate the energy required to heat or cool the house, the design temperatures and peak loads previously calculated are used with the climatic data. Table 1.11 shows the calculations for heating and cooling energy. The first three columns of the table are copied from [19] for Climate Region III. The total number of heating or cooling hours spent in each bin is calculated using equation (1.5) for cooling and (1.6) for heating. This data is used to find the number of days spent in each temperature range, shown in column four. The heating or cooling load per bin is then calculated, using the previously found peak heating and cooling loads and Eqs. (1.7) and (1.8). This is multiplied by the number of heating or cooling hours per bin to determine the total energy required to heat and cool the house in each bin, shown in column five. The total energy is divided by the number of days spent in each bin to determine how much energy is required per day to heat or cool the house. This is shown in column six. This information could then be used to analyze the selected PCM's performance.

$$f^*N_C = f^*3360 = \text{cooling hours per bin [h]} \quad (1.5)$$

$$f^*N_H = f^*4453 = \text{heating hours per bin[h]} \quad (1.6)$$

$$\dot{Q}_{heating}(T_{bin}) = \dot{Q}_{design}\left(\frac{20°C - T_{bin}}{20°C - T_{design}}\right) = 2547.39\, {kJ}/{h} \times \left(\frac{20°C - T_{bin}}{20°C - 12.8°C}\right) \quad (1.7)$$

$$\dot{Q}_{cooling}(T_{bin}) = \dot{Q}_{design}\left(\frac{T_{bin} - 23.9°C}{T_{design} - 23.9°C}\right) = 4249.89\, {kJ}/{h} \times \left(\frac{T_{bin} - 23.9°C}{31.5°C - 23.9°C}\right) \quad (1.8)$$

Table 1.11: Climate Data and Heating and Cooling Energy Required

Season	Bin Midpoint Temperature, °C	Fractional Bin Hours, *f*	Number of Days per Bin	Energy Consumption, kJ	Energy Required per Day, kJ	Percent of Energy Supplied by PCM
Cooling	38.9	0.214	30.0	6346742.5	211840.5	6.2
	36.1	0.231	32.3	5582233.5	172610.8	7.6
	33.3	0.216	30.2	4033443.8	133381.1	9.8
	30.6	0.161	22.5	2122171.4	94151.3	13.9
	27.8	0.104	14.6	799658.8	54921.6	23.9
	25.0	0.052	7.3	114237.0	15691.9	83.5
	22.2	0.018	2.5	0.0	0.0	-
Heating	19.4	0.004	0.7	769.1	1036.2	100
	16.7	0.153	28.4	176497.9	6217.4	100
	13.9	0.142	26.3	300315.7	11398.5	100
	11.1	0.138	25.6	424517.9	16579.7	79.0
	8.3	0.137	25.4	553142.2	21760.8	60.2
	5.6	0.135	25.0	674845.1	26941.9	48.6
	2.8	0.118	21.9	703300.1	32123.1	40.8
	0.0	0.092	17.1	636776.9	37304.2	35.1
	-2.8	0.047	8.7	370491.9	42485.4	30.8
	-5.6	0.021	3.9	185726.6	47666.5	27.5
	-8.3	0.009	1.7	88249.0	52847.6	24.8
	-11.1	0.005	0.9	53833.8	58028.8	22.6
	-13.9	0.002	0.4	25378.8	68391.1	19.2
	-16.7	0.001	0.2	13650.7	73572.2	17.8

On a daily basis, the maximum heating or cooling that can be compensated by the PCM is the quantity of heat that can be stored during the phase transition of the material. This heat would be stored during the day and discharged during the night, allowing that quantity of heat to be stored on a daily basis. The quantity of heat is determined by multiplying the quantity of PEG 600 in the floor with its density and heat of fusion, as shown in Eq. (1.9).

$$\text{Volume} \times \text{Density} \times \text{Heat of Fusion} = \text{Max. Thermal Storage} \tag{1.9}$$

$$79.5L \times \frac{1000cc}{L} \times \frac{1.125g}{cc} \times \frac{35cal}{gal} \times \frac{0.004184kJ}{cal} = 13{,}094kJ$$

Since this is the maximum thermal energy that could be supplied per day, this quantity is compared to the energy required per day in each temperature range bin. Column six in Table 1.11 shows how much of the energy would be supplied by the PCM for each bin. The results show that the PCM will meet the heating and cooling needs of the house for approximately 43% of the year. It is especially effective in the winter and will meet over 35% of the heating load for 91% of the heating season. Overall, the PCM will save 44.5% of the energy required to heat and cool the building. These calculations show that the addition of PCM to a building can result in significant savings in heating and cooling costs. The installed home will be monitored to determine the accuracy of these measurements, and to determine what modifications may be necessary to improve the PCMs actual performance. If auxiliary heat is needed for the exhibit, an electric resistance heater will be used.

2.4 Gray Water Recycling

Another important component of sustainability in homes is water conservation. Reducing water usage conserves this natural resource as well as saving energy to heat hot water. In a residential home, flushing the toilet and showering are two of the greatest contributors to water consumption [20]. Therefore, the focus was to reduce water usage at these two sources.

Water in homes can be reused in certain situations. Water from showers, bathroom sinks, and washers (when non-hazardous detergents are used) can be reused to flush the toilet or water a garden when treated properly. Water from these re-usable sources is called gray water, and its reuse is called gray water recycling. Water from the toilet, dishwasher, and kitchen sink (because of the potential for water contamination by food-born illnesses) contain sewage and are considered black water and cannot be reused in any situation. How gray water can be used varies by state, so the local building code should be consulted before installing any gray water recycling system [21].

In the house, the greatest quantity of water is used for the shower, as shown in Table 1.3. A very simple, inexpensive system called the AQUS is available commercially to reuse water from a bathroom sink to flush the toilet. The controls, pump, and water treatment are integrated into the system [22]. In the house, there is no bathroom sink, but there is sufficient water used in showering to flush the toilet. The AQUS system was adapted to sit underneath the floor and collect the shower gray water to flush the toilet. Using a 6 liter energy conserving water toilet, and estimating 6 uses per day, This saves 36 liters of water daily. The AQUS is located underneath the kitchen cabinets, so as to be visible to the public, as well as to allow easy access for maintenance.

Other strategies for conserving water include using a low flow showerhead (1.5 gpm /.095 L/s), a water-conserving toilet which only uses 6 L (1.6 gal) per flush, and an aerator for the kitchen sink (1.5 gpm /.095 L/s). The low-flow water fixtures and aerators are a simple and inexpensive sustainable strategy for homeowners to employ. In this way the house displays a wide range of strategies for homeowners to implement in their own homes – from simple and inexpensive to more complicated and requiring a larger initial investment.

3. Conclusions

Residential buildings consume 19.6% of the energy used by the United States, demonstrating the importance of improving residential building technology and homeowner awareness of these technologies. The house accomplishes this by incorporating as many sustainable technologies as possible into the house design, and by being installed as an exhibit at COSI. The technologies incorporated in the home result in significant energy savings. Solar power generation and solar hot water heating will meet the needs of two theoretical residents. The 386 W rated photovoltaic array will produce 380 kWh annually. The solar hot water collector will meet the 17,395 kW demand with very little auxiliary heat required. SIPs, energy star windows, and the PCM incorporated in the floor will reduce the peak heating and cooling load. The PCM is estimated to reduce the energy required to heat and cool the house by 44.5% annually. Significant water savings are also achieved through the use of an innovative gray water recycling system and low flow fixtures. The operation of each of these systems will be monitored during its installation to determine its actual performance and to suggest modifications. The home realizes its goal of successfully implementing sustainable strategies in a unique home that displays current and innovative technology both as a test platform and to raise homeowner awareness.

4. Project Acknowledgements

The author would like to thank Doug Powell for his contribution to this paper. This project would not have been possible without the generous support of The Ohio State University College of Engineering, specifically the Department of Mechanical Engineering, the Department of Food, Agricultural and Biological Engineering and the Knowlton School of Architecture and contributions from the Center of Science and Industry, The Ohio State University 2009 Solar Decathlon Team, The Ohio State University Center of Automotive Research, Columbia Forest Products, S.U.N./Equinox, Fantech, Ohio Radiant Floor, Inc, and Mr. Don Evanoo.

5. References

[1] 2009, “Annual Energy Review 2008”, Energy Information Administration, United States Government Printing Office, p. 3, http://www.eia.doe.gov/emeu/aer/contents.html.

[2] Marion, W. & Wilcox, S., 1994, “Solar Radiation Data Manual for Flat-Plate and Concentrating Collectors”, National Renewable Energy Lab, p. 3, http://rredc.nrel.gov/solar/pubs/redbook/.

[3] 1994, “30 Year Average of Monthly Solar Radiation, 1961-1990”, National Renewable Energy Lab Renewable Resource Data Center, http://rredc.nrel.gov/solar/old_data/nsrdb/redbook/sum2/state.html

[4] 2008, “PV Watts Version 1 Calculator,” National Renewable Energy Lab Renewable Resource Data Center, http://rredc.nrel.gov/solar/calculators/PVWATTS/version1/

[5] 2009, “Average Retail Price of Electricity to Ultimate Customers: Total by End-Use Sector”, Electric Power Monthly, No. DOE/EIA-0226 (2009/12), Energy Information Administration, p. 104, http://www.eia.doe.gov/cneaf/electricity/epm/epm.pdf

[6] Lutz, J. D., Liu, X., McMahon, J. E., Dunham, C., & McGrue, Q. T., 1996, "Modeling Residential Hot Water Use Patterns," No. LBL-37805, Lawrence Berkeley National Laboratory.

[7] “SOLARHOT Platinum Series,” SolarHOt, Morrisville, NC, http://www.solarhotusa.com/support/literature/files/collector.pdf

[8] Energy Information Administration, 2009, “Annual Ohio Price of Natural Gas Delivered to Residential Consumers,” http://tonto.eia.doe.gov/dnav/ng/hist/n3010oh3a.htm.

[9] Christian, J., Desjarlais, A., & Kosny, J., 1999. “Whole Wall Rating/Label for Structural Insulated Panels: Steady-State Thermal Analysis,” Oak Ridge National Laboratory Buildings Technology Center, http://www.sips.org/elements/uploads/files/fileManager/WholeWallR-ValueStudy.pdf

[10] Arif, M. & Mullens, M.A., 2006, “Structural Insulated Panels: Impact on the Residential Construction Process,” Journal of Construction Engineering and Management, 132(7) pp. 786-795.

[11] 2005, “The Facts About Solar Heat Gain & Windows,” National Fenestration Rating Council, http://www.nfrc.org/documents/U-Factor.pdf

[12] 2005, “The Facts About Windows & Heat Loss,” National Fenestration Rating Council, http://www.nfrc.org/documents/U-Factor.pdf

[13] 2007 ASHRAE Handbook - Heating, Ventilating, and Air-Conditioning Applications (I-P Edition), American Society of Heating, Refrigerating and Air-Conditioning Engineers, Inc, pp. 34.1-34.2.

[14] Sharma, S.D. & Sagara, K., 2005, “Latent Heat Storage Materials and Systems: A Review,” International Journal of Green Energy, 2, pp. 1-56.

[15] Zhang, Y., Zhou, G. , Lin, K., Zhang, Q., & Di, H., 2006, “Application of Latent Heat Thermal Energy Storage in Buildings: State-of-the-Art and Outlook,” Building and Environment, 42, pp. 2197-2209.

[16] 2007, “Polyethylene Glycol 600,” MSDS No. UCN0038E (2007), Univar USA Inc, Redmond, WA.

[17] 2006, “CARBOWAX Polyethylene Glycols and Methoxypolyethylene glycols,” Dow Chemical Company: Midland, MI, http://www.dow.com/polyglycols/carbowax/resource/index.htm

[18] 2009 ASHRAE Handbook - Fundamentals (I-P Edition), American Society of Heating, Refrigerating and Air-Conditioning Engineers, Inc, pp.17.1-17.16.

[19] Watson, R.D. & Chapman, K. S., 2002, Radiant Heating and Cooling Handbook, McGraw-Hill, New York, NY, pp. 4.1-4.8.

[20] 2006, “The Department of Natural Resources Division of Water Fact Sheet: Efficiency at Home,” Ohio Department of Natural Resources Division of Water, Columbus, Ohio, http://www.dnr.state.oh.us/Portals/7/pubs/pdfs/fctsht01.pdf

[21] Rozgus, A., 2009, “Using Gray Water Efficiently,” Consulting-Specifying Engineer, 45(3), p. 19-20.

[22] 2008, “AQUS System Specifications,” WaterSaver Technologies, Louisville, KY, http://www.watersavertech.com/AQUS_Specifications_Sheet.pdf

Chapter 2:

Numerical Simulation of the 2009 Ohio State University Solar Decathlon House Thermal Storage Wall Incorporating Phase Change Material

Abstract

The 2009 Ohio State University Solar Decathlon house included a thermal storage wall incorporating phase change material (PCM). The actual thermal storage wall consisted of shading devices, Polygal glazing, and a thermal storage element consisting of Polyethylene Glycol 600 encapsulated in clear polycarbonate tubes. Finite element analysis was used to evaluate the effectiveness of the thermal storage wall design. The performance of the wall was evaluated with and without the inclusion of PCM. In addition, polycarbonate and aluminum container materials were evaluated. Results indicated that the PCM very effectively moderated the heat transfer through the wall. No conclusive performance difference between the polycarbonate and aluminum containers was found. However, the aluminum container did improve the heat cycling between the PCM and its surroundings. The results suggested several beneficial improvements to the original thermal storage wall design.

1. Introduction

Recent national awareness of the finite availability of fossil fuels and their negative impact on the environment has led to a renewed interest in energy efficiency and conservation. In the U.S., residential buildings account for 21.8% of the overall energy used, which at more than commercial buildings, industry, and transportation sectors [1], makes the improvement of energy-efficiency in residential buildings an important national issue. Of the total energy used by residential buildings, 40.8% is consumed by space heating, which is significantly more than that used by air-conditioning, water heating, appliances and lighting [2]. Decreasing the energy required to heat the home would have the largest impact on residential energy efficiency.

1.1 Sensible vs. Latent Heat Storage

The renewable energy of the sun can be used to reduce energy consumption of a building by passive heating. One way to accomplish passive heating is to store the sun's heat in a thermally massive material, such as concrete or brick. This is an example of *sensible heat storage*, when a material stores heat by increasing in temperature. The amount of heat stored is dependent upon the heat capacity, c_p, and the mass of the storage medium, and the temperature change of the material as shown in Eq. (2.1) [3].

$$Q = m \cdot c_p \cdot \Delta T \tag{2.1}$$

There are two main benefits to increasing the thermal mass of a building [4]. Thermal mass will moderate the peak heating and cooling loads of a building throughout the day, which decreases peak heating loads saving costs both in energy and equipment sizing. Thermal mass will also delay the peak heating and cooling loads to a later time. In places where peak vs. off-peak electricity costs are different, shifting peak heating and cooling times can result in lower energy costs.

Unfortunately, most thermally massive materials must be very heavy to be effective, and thus result in very thick walls or floors. For lightweight construction, the most common building method for residential buildings, the application of a phase change material (PCM) can be a more effective solution. An appropriately selected material will store a significant amount of the sun's energy as it melts without increasing in temperature. This method of storage is called *latent heat storage* and the amount of heat stored is based upon the mass of the material, the fraction of material melted, f_m, and its heat of fusion, h_f, as shown in Eq. (2.2) [3].

$$Q = m \cdot f_m \cdot h_f \tag{2.2}$$

Since $h_f >> c_p$, a much lower mass of material can be used to obtain the same heat storage, as long as a significant portion of the material is melted.

Research has been done to quantitatively compare the effectiveness of latent heat storage versus sensible heat storage with traditional building materials. Table 2.1 compares the heat storage capacity and density of some common building materials with that of PCM. When applied at the melting point of the PCM, the significant increase in energy storage from latent heat is easily shown [5].

Table 2.1: Heat Capacities and Heat Stored per Volume in a 4˚K Temperature Interval for Different Building Materials and PCMs

	Material	c_p [kJ/kg-K]	h_f [kJ/kg]	ρ [kg/m^3]	Q/V for ΔT=4˚K [MJ/ m^3]
Building Materials	Gypsum	0.8	-	800	2.56
	Wood	1.5	-	700	4.20
	Concrete	0.84	-	1600	5.38
	Sandstone	0.7	-	2300	6.44
	Brick	1	-	1800	7.20
PCM	Salt Hydrate: $CaCl_2{\cdot}6H_2O$	-	192	1562	300
	Paraffin: Heptadecane	-	215	778	167
	PEG 600	-	146	1126	164

1.2 Historical Background

The use of PCMs for thermal storage in buildings was originally investigated by Telkes in 1978 [6]. Telkes used active storage of solar energy into Glauber's salt ($Na_2SO_4{\cdot}10H_2O$). Initially only Glauber's salt was considered as a potential phase change material, but observations showed that is suffers from subcooling and separation after very few cycles. Glauber's salt has continued to be investigated as attempts have been made to resolve the subcooling and separation issues [7-9].

Telke's original work opened the door for many other materials to be investigated for their potential application in buildings. The first comprehensive list of suitable PCMs was compiled by Lane in 1983 [3] and 1986 [10], and was updated by Khudhair and Farid in 2004 [11] and Zhang et al in 2007 [12]. Table 2.2 shows the list of PCMs for building applications given by Zhang et al.

Table 2.2: PCMs Suitable for Passive Solar Applications in Buildings

Classification	PCM	Melting Temperature [˚C]	Heat of Fusion [kJ/kg]
Inorganic Salt Hydrate	$CaCl_2 \cdot 6H_2O$	24-29	192
	$Na_2S_2O_3 \cdot 5\ H_2O$	40	210
Organic Paraffin	Hexadecane	18	236
	Heptadecane	22	214
	Octadecane	28	244
	Black Paraffin	25-30	150
Organic Non-paraffin	1-dodecanol	26	200
	Polyethylene Glycol (PEG) 600	15-25	150.5
	Propyl Palmitate		
	Butyle Stearate	19	140
Eutectic Organic-organic	Butyle Stearate + Butyl Palmitate (50/48)	18-22	140
	Capric-lauric (45/55)	21	143
	Capric-lauric (82/18)	19.1-20.4	147
	Capric-lauric (61.5/38.5)	19.1	132
	Capric-myrstic (73.5/26.5)	21.4	152
	Capric-palmitate (75.2/24.8)	22.1	153
	Capric-stearate (86.6/13.4)	26.8	160

A list of PCMs for any temperature application as well as a list of commercially available PCMs was developed by Sharma and Sagara in 2005 [13]. Most recently, Mehling and Cabeza published a comprehensive textbook introducing the reader to the science behind PCMs and their application for heat and cold storage [5].

1.3 PCM Selection

The selection of an appropriate PCM is vital to the successful performance of a latent heat storage system. Most PCMs can be classified as one of three types: Organics, Inorganics, and Eutectics. These can further be broken-down into various subcategories. Figure 2.1 shows the classes of PCM materials [13].

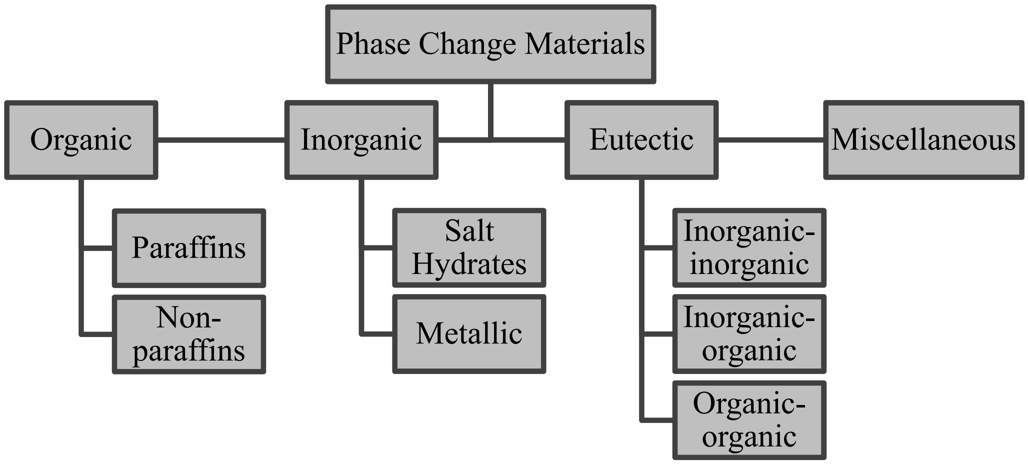

Figure 2.1: Classifications of PCM Materials

Each PCM type has its own advantages and disadvantages. Organic paraffins are the most common commercially used PCM. They are waxy liquids or solids which are safe to handle and very stable. They have a very high heat of fusion, but a low thermal conductivity. Unfortunately, they are also extremely flammable, which has caused them to be unfavorable for residential applications. Non-paraffins are the largest class of PCM materials. Their properties vary widely, depending on the material [12]. Hydrated salts are the most common inorganic PCM. They are attractive because they have high heats of fusion, high thermal conductivity, are non-flammable and inexpensive. However, they are generally corrosive and incompatible with many types of containers or building materials. They often experience phase segregation during transition and require the use of nucleating and thickening agents, complicating their application. Eutectic materials are mixtures of two or more PCMs to achieve the desired melting point and material properties [13].

Sharma and Sagara give an outline for the properties that should be considered when choosing an appropriate PCM for a particular application. Most importantly, the melting temperature must be in the desired operating range. A high latent heat of fusion per unit volume is desirable so that a smaller mass of material will store the required amount of heat. A high specific heat will provide additional significant heat storage above or below the melting point of the material. A small volume change upon melting and solidification will simplify container design. Chemically, the material should be stable and see no degradation after a large number of freeze/melt cycles, such as phase segregation. The affects of subcooling should also be considered. For building applications, it is important that the PCM be completely safe, especially in regard to flammability and toxicity. The material must also not react with the container or building materials it will come in contact with, causing damage to the PCM or the container. Also importantly, the material must be readily available at a reasonable cost to be economically viable [13]. Unfortunately no PCM will have the perfect combination of desired attributes. Although all of these requirements are important, the best PCM is selected based upon the individual needs of an application.

1.4 PCM Incorporation Method

The most challenging aspect of applying PCMs to buildings is the method of incorporation into the building. There are three methods for effectively integrating PCMs into buildings: Direct incorporation, encapsulation, and shape stabilization. Direct incorporation is the cheapest and easiest method, where a PCM is mixed directly into the building material during production or the building material is immersed in the PCM after production. However, direct incorporation is prone to leakage of the PCM over time [12].

Encapsulation can be done on both the macro and micro scale. Micro-encapsulation involves mixing very small volumes or particles of PCM which have been coated by an outer encapsulation material directly into the building material. A large amount of research has been conducted on incorporating PCM directly into building materials by mixing the PCM directly into the material, or mixing a micro-encapsulated PCM directly into the material. In 1991, Pieppo et al conducted a theoretical simulation to study drywall impregnated with PCM and suggested criteria for selecting the optimal PCM [14]. Scalat et al followed this in 1996 with full-scale testing that showed the PCM wallboard maintained the room temperature for several hours after the HVAC system was shut off [15]. In 2000 Neeper showed that for PCM wallboard diurnal energy storage decreases if the PCM melts over a range of temperatures and also that storage may be limited to 300-400 kJ/m^2 even if the wallboard has a greater latent heat capacity [16]. Voelker et al in 2008 studied micro-encapsulated paraffin and salt-hydrate in wallboard and proved that PCMs forfeit their characteristic heat storage after a few consecutive hot days if they cannot discharge overnight [17]. In 2009, Castellón et al studied concrete and brick impregnated with PCM in 9 small test buildings, and showed that in the buildings with PCM temperature oscillation was reduced by 4˚C, and peak temperatures were shifted to later hours [18].

The second form of encapsulation is macro-encapsulation. This involves containing the PCM in pouches, tubes, spheres or other shaped receptacles, which are then incorporated into the building. Although incorporating containers into a building requires more initial effort in the design and installation [12], it is the most widely used type of commercial encapsulation [3]. Considering the widespread use of macro-encapsulation for PCMs, it is surprising that there is very little published work discussing its application. However, some information is available. In 1983, Knowles studied the heat resistance of thermal storage walls using both traditional materials and macro-encapsulated paraffin. His research found that dispersing a metallic component in the paraffin could successfully improve the thermal conductance of the latent heat wall, making it more effective [19]. Benard et al compared a concrete wall to hard and soft paraffin latent heat storage walls and found that paraffin, at 1/12 the weight, performed similarly to concrete [20]. More recently, commercial pre-fabricated walls encapsulating PCM were studied in 2006 by Carbonari et al [21] and Ahmad et al 2006 [22]. Integration of PCMs into building structures is simple to achieve with commercial walls that have macro-encapsulation of PCM.

Lane et al detail the important considerations when designing a container for PCM storage [3]. The container must be compatible with the PCM, especially in regard to corrosion. For example, salt hydrates are commonly held in plastic containers because they react with many common metals. The container must also be able to withstand any mechanical stress on the container walls induced by volume change of the melting PCM. Finally, the container must be sealed to prevent moisture from contaminating salt hydrates and/or to act as a barrier against vapors from organic PCMs . Also, since many PCMs suitable for passive solar applications have low thermal conductivities, the ideal container will allow for easy heat transfer between the ambient air, container and PCM. All of these constraints must be taken into consideration when designing a container for macro-encapsulation.

1.5 Passive Solar Heating in Buildings

There are two common methods of applying passive solar heating to buildings. These can be classified as direct or indirect gain methods. In direct gain, windows on the south side of a building allow solar radiation to directly heat a room with extensive thermal mass inside the building envelope. With indirect gain, external building elements absorb solar radiation and transmit it into the room. One of the most common methods of applying indirect gain solar heating to a building is to include a thermal storage wall (TSW) on the south side of the building. A TSW consists of glazing, an air gap, and a thermally massive wall as the thermal storage element, as shown in Figure 2.2. Usually, an overhang is designed into the wall to prevent summer sun from striking the TSW, but to allow the winter sun to heat the system.

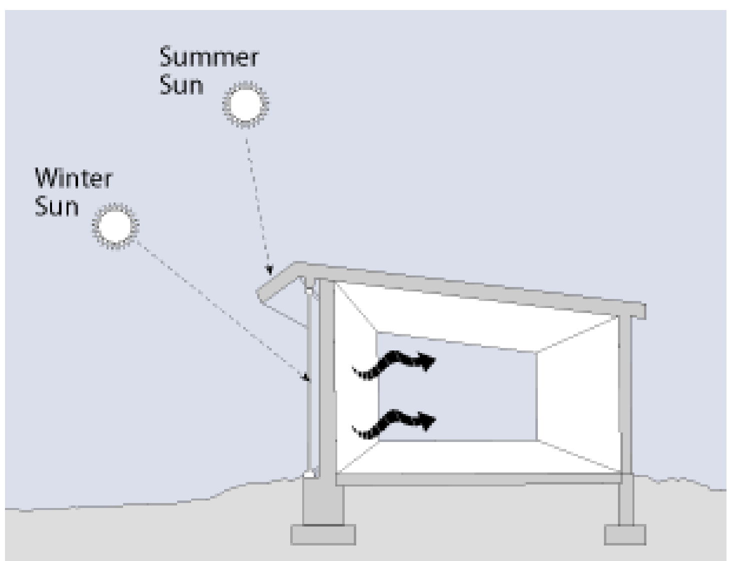

Figure 2.2: Components of a Thermal Storage Wall System

The TSW operates by solar radiation striking a high-performance glazing, which transmits as much of the radiation as possible into the air space. The solar radiation will strike the surface of the thermal storage element and become heat, some of which is stored in the wall and some of which is stored in the air space. The high-performance glazing will prevent the heat trapped in the airspace from being transmitted back to the exterior. The thermal storage element will then be heated by both the solar radiation and the heat trapped in the air space. Although the thermal storage element traditionally consists of sensible heat storage using concrete or brick, this is an excellent application of latent heat storage materials. For more information on the design of passive solar heating systems in residential homes, refer to Lebens [23] and Steven Winter Associates, Inc [24].

1.6 Investigation Goals

The 2009 Ohio State University Solar Decathlon Team included a thermal storage wall incorporating phase change material into the southern façade of the house. The purpose of this study is to use finite element analysis (FEA) to evaluate the effectiveness of the thermal wall design. The effectiveness of the PCM as a thermal storage element is evaluated for circular polycarbonate and aluminum containers and is compared to an empty wall with no PCM. Polycarbonate is the material used for the containers in the Solar Decathlon house, but aluminum is hypothesized to be a more effective container material by improving the conductivity of the container. This would allow for more effective heat transfer between the PCM and its surroundings. Each of these cases is modeled for a representative severe, moderate, and mild winter day to illustrate the wall's heat storage performance during the winter months.

2. The OSU Thermal Storage Wall

The purpose of the theoretical model is to evaluate the performance of the 2009 Solar Decathlon team's thermal storage wall incorporated into the southern façade of the house. The wall consisted of 2 layers of semi-translucent plastic glazing, separated by a 5.25" air gap containing polycarbonate tubes filled with PCM. Figure 2.3 shows a picture of the thermal storage wall open from the interior to show the PCM filled polycarbonate tubes.

Figure 2.3: Thermal Storage Wall Open to Show PCM-filled Polycarbonate Tubes

2.1 House Materials

The PCM selected for use in the Solar Decathlon house was Polyethylene Glycol 600 (PEG 600). Polyethylene glycol has several properties that make it ideal for building applications. PEG 600 changes phase over the temperature range of 15° - 25° C, so it will store heat at room temperature. It has a large heat of fusion of 146.4 kJ/kg. When it melts, PEG 600 has not shown any tendencies to experience phase segregation or subcooling [10]. It will not react with most container materials, including glass, metals, and many plastics. PEG 600 is readily available from Dow Chemical under the trade name CARBOWAX 600, for approximately $3.25/kg (Univar USA, 2009). Perhaps most importantly, PEG 600 is an extremely safe chemical. OSHA considers it non-hazardous and it has NFPA ratings of 1 for Health, 1 for Fire, and 0 for Reactivity. It is often used for pharmaceutical and personal care products, further underscoring its safety [25].

The macro-encapsulation method for the PEG 600 was chosen with input from both engineering and architecture students on the Solar Decathlon team. It was desirable to have a clear container to allow as much natural light as possible to reach the interior of the house. The polycarbonate tubes met this design requirement while allowing for a large amount of PCM to be stored in the cavity. Unlike traditional thermal storage walls, instead of the PCM directly transmitting the stored heat into the room, the air in the cavity is the medium used to transfer heat to and from the PCM. The glazing material is Polygal Thermogal, a well-insulating material with 54% light transmission and a U-value of 1.7 W/m^2-K [26]. This U-value is similar to that of high performance double pane glass windows. A cross section of the thermal storage wall is shown in Figure 2.4.

INTERIOR

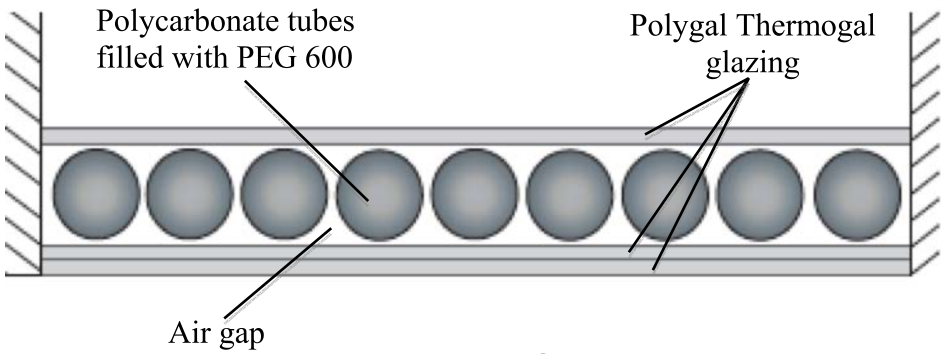

EXTERIOR

Figure 2.4: Cross Section of Thermal Storage Wall

2.2 Model Development

The analysis of a solid-liquid phase transition is traditionally known as the Stefan problem, after Joseph Stefan who first analyzed the process in 1891 [5]. Unique to the Stefan problem is the non-linearity caused by the moving solid-liquid interface as the material undergoes melting or solidification. There are two models for solving heat transfer in a solid-liquid phase change. The temperature-based method can be applied to substances with a discrete melting temperature and sharply defined interface. The enthalpy-based method is applied to problems where materials change phase over a range of temperatures, resulting in a two-phase, “mushy” region between the solid and liquid phases. In this case, enthalpy and temperature are both dependent variables, and the solution does not track the position of the interface explicitly. The enthalpy-based method is considered the weak form of the Stefan problem. Although both analytical and numerical solutions of the Stefan problem are available, accurate analytical solutions are often difficult to obtain because of the non-linearity of the problem due to the moving solid-liquid interface [3].

For evaluation of the Solar Decathlon house thermal storage wall, a numerical analysis using FLUENT was conducted. To solve melting and solidification based problems, FLUENT uses a version of the enthalpy-based method developed by Voller and Prakash in 1987 called the enthalpy-porosity formulation [27]. Since the PCM used in the thermal storage wall does not have a sharply defined melting temperature, numerical evaluation must be done using the enthalpy-based method. In the enthalpy-porosity formulation, the liquid-solid transition region is treated as a porous area, with the porosity equal to the fraction of melted material in the two-phase zone. Each cell of the mesh has an associated liquid fraction value equal to the fraction of cell area that is in liquid form. Therefore, in the transition zone the liquid fraction will have a value between 0 and 1, with the value decreasing to zero as the material solidifies. In FLUENT, there is a linear relationship between the temperature and the liquid fraction, which is evaluated at each iteration based on an enthalpy balance of the energy equation. Once the upper and lower bounds of the melting temperature are identified as $T_{solidus}$ and $T_{liquidus}$ respectively, the melting fraction is evaluated as shown in Eq. (2.3).

$$\begin{aligned} &f_m = 0 \ \text{ if } \ T < T_{solidus} \\ &f_m = 1 \ \text{ if } \ T > T_{liquidus} \\ &f_m = \frac{T - T_{solidus}}{T_{liquidus} - T_{solidus}} \ \text{ if } \ T_{solidus} < T < T_{liquidus} \end{aligned} \tag{2.3}$$

The latent heat, ΔH_l, stored in each cell is then calculated using the liquid fraction and latent heat of the material, as shown in Eq. (2.4).

$$\Delta H_l = f_m \cdot h_f \tag{2.4}$$

The total enthalpy of each cell is required to balance the energy equation. The total enthalpy, H, is the sum of the sensible enthalpy, h, and the latent heat as shown in Eq. (2.5).

$$H = h + \Delta H_l \tag{2.5}$$

The equation for the evaluation of sensible enthalpy is shown in Eq. (2.6). The sensible enthalpy is the sum of the initial enthalpy of the material, h_i, and the heat stored sensibly in the material due to the change in temperature [28].

$$h = h_i + \int_{T_i}^{T} c_p dT \tag{2.6}$$

Another important component of the energy equation is the fluid velocity vector, $\vec{v}$, introduced by buoyancy-driven natural convection. The velocity of the fluid component of the domain is accounted for in the energy equation, but to account for velocity in the transition region of the domain, a momentum source term is added to the energy equation. The momentum source term, S, accounts for the velocity in the transition region of the material, and is evaluated as shown in Eq. (2.7).

$$S = \frac{(1 - f_m)^2}{(f_m^{\ 3} + \varepsilon)} \cdot A_{mush} \cdot \vec{v} \tag{2.7}$$

A_{mush} is the transition zone constant, and ε is a small number required to prevent division by zero. The transition zone constant measures the momentum damping as the material solidifies. The higher this value, the faster the velocity will transition to zero as the material solidifies. The above quantities are then used to evaluate the energy equation, written in Eq. (2.8). FLUENT solves for the temperature at each time step by iterating between the energy equation and the liquid fraction equation [28].

$$\frac{\partial}{\partial t}(\rho H) + \nabla \cdot (\rho \vec{v} H) = \nabla \cdot (k \nabla T) + S \tag{2.8}$$

2.3 Numerical Model Setup

The thermal performance of the wall was evaluated using a 2D FEA analysis in FLUENT. The 2D shape used is a representative cross section of the thermal storage wall, as shown in Figure 2.5. It includes a single tube of PCM with the interior and exterior glazing. Symmetry is applied to the east and west wall boundaries of the cross section, simulating a continuous thermal storage wall with repeating tubes. This will approximate the actual repeating pattern of tubes in the Solar Decathlon thermal storage wall. Figure 2.5 also indicates the labels used to identify the surface zones and boundaries of the mesh. The overall dimensions of the cross section are 208 mm long by 127 mm wide. Each layer of Polygal is 25 mm thick. The circular container has an outer diameter of 114 mm (4.5 in) with a wall thickness of 106 mm (.125 in) and is centered in the air space.

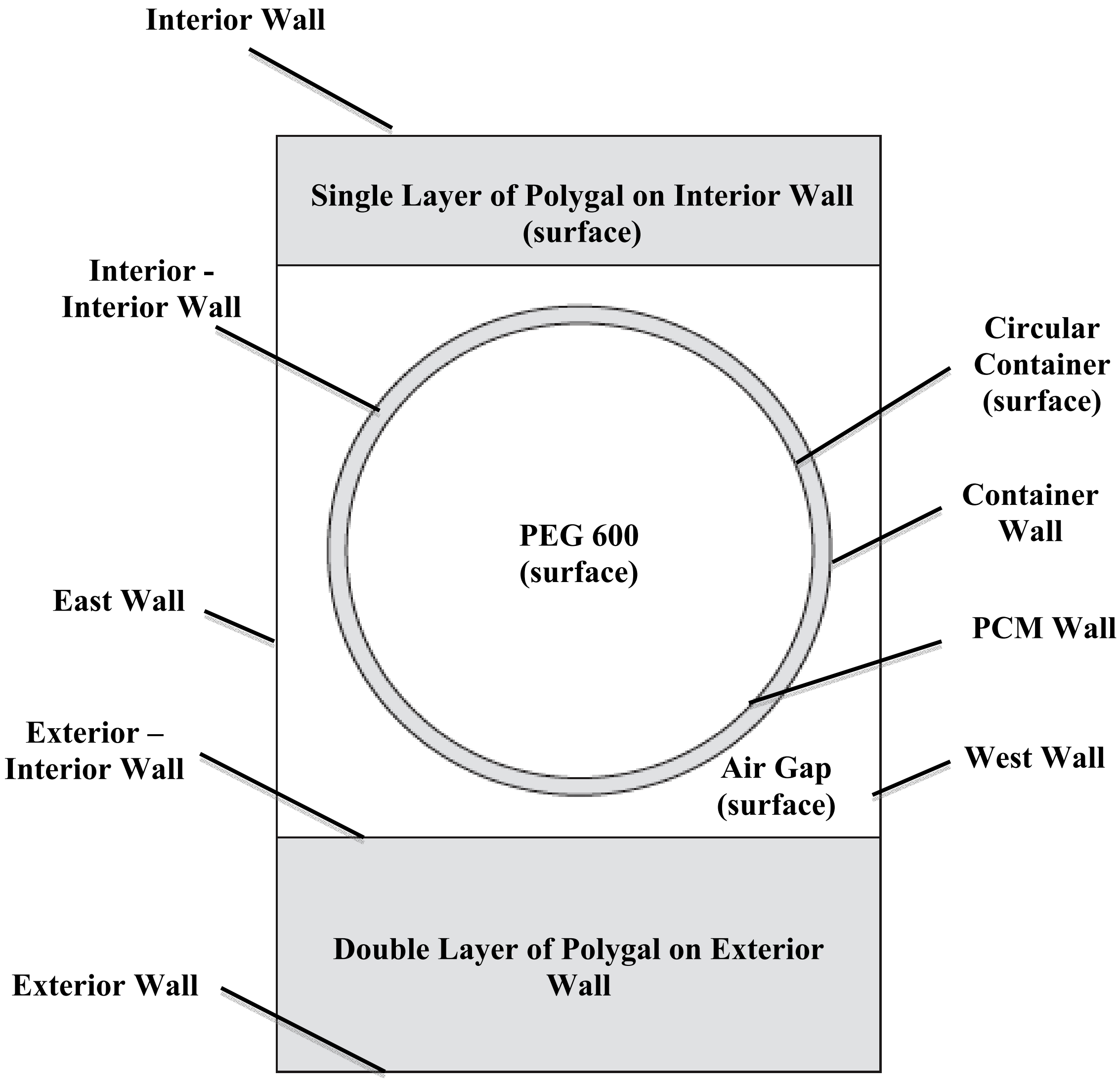

Figure 2.5: Cross Section of Thermal Storage Wall Cavity for FEA Analysis

Figure 2.6 shows the meshed cross section. Quadrilateral cells were used to improve accuracy and decrease run time. The total of 4,217 elements were in the mesh with 4,728 nodes. The average mesh size was 2.5x 2.5 mm.

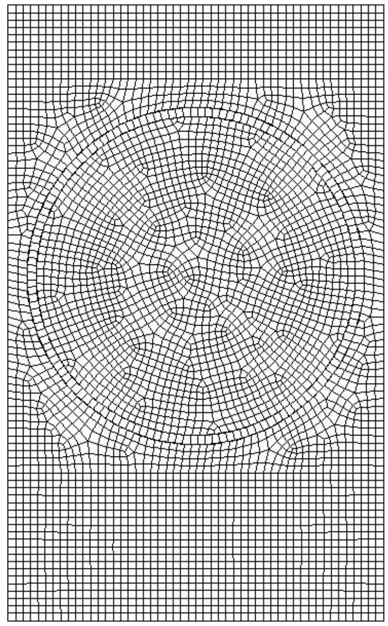

Figure 2.6: Meshed Thermal Storage Wall Cross Section

After meshing the surface, material properties and boundary conditions were applied to the model. For all materials, density, specific heat, and thermal conductivity were input to FLUENT. For the PEG 600, the heat of fusion and solidus and liquidus temperatures bounding the melting range were also entered. Both aluminum and polycarbonate were used as the container material. Boundary conditions were applied to each wall of the mesh to simulate actual operating conditions. The east and west walls are both symmetry conditions, to simulate the repeating tube pattern in the wall. The interior wall has a convection boundary condition to an unchanging temperature of 293 °K (67.7 °F), with a convection coefficient of 50 W/m^2. This is the minimum temperature that is still within the comfort zone for a home [29].

For the external wall and external-interior wall, boundary conditions are applied to simulate actual temperature and solar radiation conditions for representative mild, moderate, and severe winter days in Columbus, Ohio. November 15, December 15, and January 15 represent mild, moderate and severe winter days, respectively. Historical temperature and solar radiation data are available for Port Columbus International Airport. The hourly solar radiation data is published by the National Renewable Energy Lab Renewable Resource Data Center (RReDC) for the years 1991-2005 in their National Solar Radiation Database [30], and the temperature data from Port Columbus is available online [31]. The temperature and solar radiation data were collected for the years 1995-2005, and averaged to give a representational 10-year hourly value. Figure 2.7 shows the 10-year average value of temperature for November 15, December 15 and January 15. Figure 2.8 shows the 10-year average value of global horizontal solar radiation.

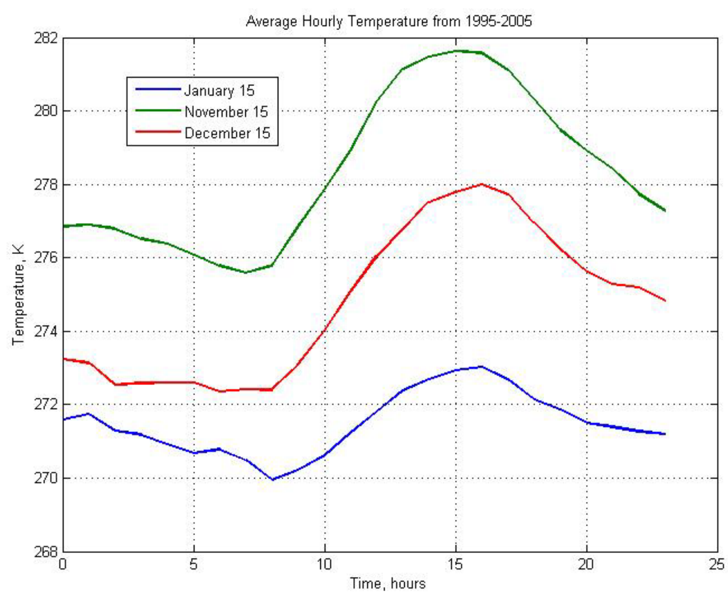

Figure 2.7: 10-year Average Hourly Temperature

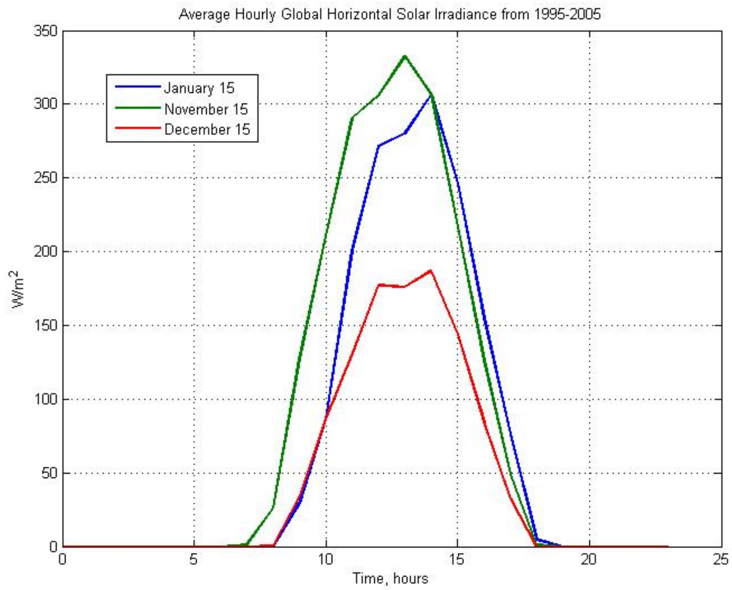

Figure 2.8: 10-year Average Hourly Global Horizontal Solar Radiation

To model the change in temperature with time in FLUENT, a sinusoidal function was used. The sine wave was centered on the daily average temperature with amplitude equal to half of the difference between the daily max and min temperature. The hottest point of the day occurred at approximately 16 hours, so the max value of the sinusoid was translated to match. Table 2.4 gives the daily average and change in temperature values and the resulting equation used to model the temperature in FLUENT.

Table 2.3: Daily Average, Minimum, and Maximum Temperatures used to Develop a Sine Wave Approximation for Temperature as a Function of Time

Day	Average Temperature, K	Change in Temperature, K	Sinusoidal Approximation Function, f(t)
Mild, November 15	278.3	6.05	$f(t) = \frac{6.05°C}{2} \cdot \sin\left(\frac{2\pi t}{24} + 10\right) + 278.3°C$
Moderate, December 15	274.8	5.64	$f(t) = \frac{5.64°C}{2} \cdot \sin\left(\frac{2\pi t}{24} + 10\right) + 274.8°C$
Severe, January 15	271.5	3.09	$f(t) = \frac{3.09°C}{2} \cdot \sin\left(\frac{2\pi t}{24} + 10\right) + 271.5°C$

To approximate the component of heat added to the thermal storage wall from solar radiation, it was necessary to determine what fraction of the solar radiation would be transmitted through the Polygal glazing and result in heat added to the air gap. In 2008, Ismail et al developed Eq. (2.9) to determine the fraction of solar radiation, *F*, directly transmitted through a window system [32]. The equation determines how much solar radiation penetrates directly, and how much is absorbed by the glazing system and is directed to the interior by heat transfer.

$$F = \tau + \alpha \cdot \frac{U}{h_{ext}} \tag{2.9}$$

In this (Eq 2.9), τ is the fraction of incident solar radiation directly transmitted through the window system, α is the fraction of radiation absorbed, U is the overall heat transfer coefficient of the wall system, known as the U-value, and h_{ext} is the convection coefficient to air from the wall. Therefore, the quantity $\alpha U/h_{ext}$ is the fraction of solar radiation that is absorbed by the window system but then transmitted as heat. For Polygal ice, the U-factor is given as 1.7 W/m^2-K, and 54% of the light is transmitted [26]. However, the exterior glazing window system is two layers of Polygal. For a two-layer system, Eq. (2.9) is adjusted as shown in Eq. (2.10).

$$F = \tau^2 + 2\alpha \cdot \frac{U}{h_{ext}} \tag{2.10}$$

Because no data is given on the reflective or absorptive properties of Polygal, it was assumed that, of the 54% of light transmitted, half of the remaining solar radiation is absorbed and half is reflected. This results in a value of α equal to 23%. Combining this information, it was found that 30.7% of the solar radiation would result in heat. To find the solar radiation as a function of time, MATLAB was used to fit a fourth order polynomial to the solar radiation data. Figure 2.9 shows the 10-year average solar radiation and the fitted curves.

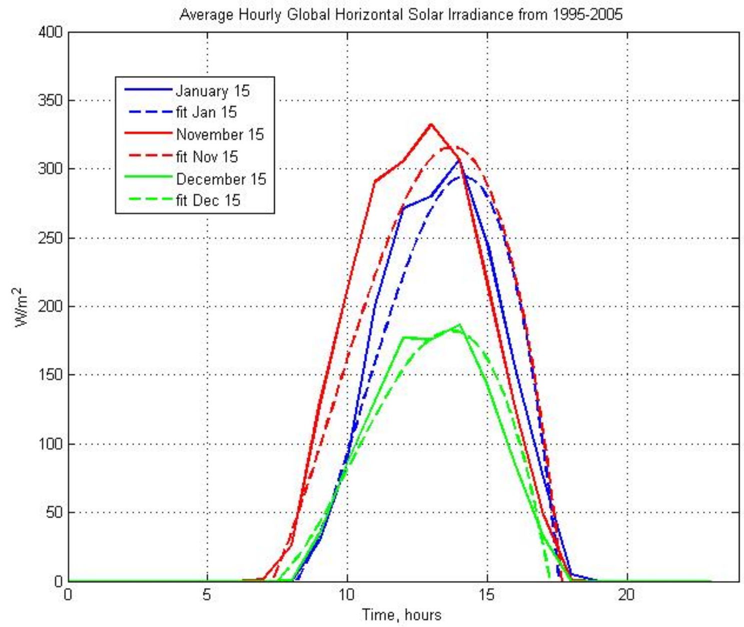

Figure 2.9: 10-year Average Solar Radiation Data and Polynomial Curve Fits

To determine how much heat was added to the wall from solar radiation, the solar radiation polynomial was multiplied by the solar radiation heat gain fraction. There is zero heat generation from solar radiation applied to the boundary at times before sunrise or after sunset.

3. Results and Discussion

FLUENT was used to model representative mild, moderate and severe winter days. The initial temperature of the entire model was set at 293 °K, which corresponds to the interior temperature of the house. Since the interior temperature is maintained year-round at 298 °K, it is assumed that 298 °K is a reasonable initial starting condition. The model performs one-hour time steps, for a total of 120 hours, or five days. It is unlikely that Ohio would see more than five consecutive sunny days in the winter, so five days would sufficiently model the effects of solar radiation on wall performance. Also importantly, simulating five days allows sufficient time for trends to appear in the data. As previously mentioned, the following three simulations were performed: polycarbonate containers, aluminum containers, and PCM within the wall. Outputs from the model included the PCM area-average liquid fraction, the average heat flux across the interior-interior wall, and the area-average air gap temperature. Using plots of these parameters, the performance of the thermal storage wall is evaluated.

Figure 2.10 shows a plot of the liquid fraction of the phase change material vs. time for both the aluminum and polycarbonate containers. The liquid fraction indicates the fraction of PCM melted. Examination of the plot of liquid fraction vs. time shows when the PCM is absorbing or releasing heat. A positive slope indicates heat is beings absorbed, while a negative slope indicates heat is being released. The slope also indicates the rate at which heat is being absorbed or released, with a steeper slope showing that heat is being transferred more quickly. Because the initial temperature of the PCM at t=0 is 293 °K, the PCM is approx. 50% melted at the beginning of the simulation.

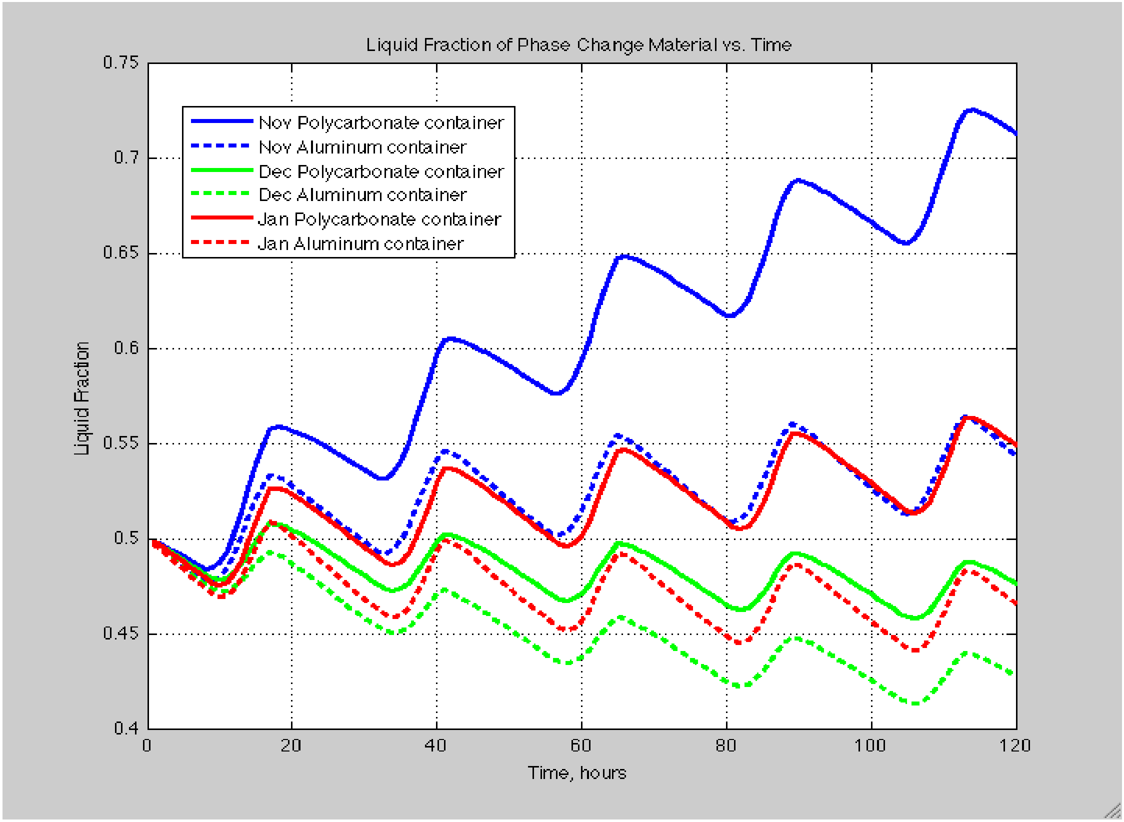

Figure 2.10: Liquid Fraction of Phase Change Material vs. Time

Figure 2.10 shows that the liquid fraction for polycarbonate containers is always greater than that for aluminum containers. This is because the aluminum is better at conducting the heat out of the tube, while the polycarbonate insulates the PCM, preventing the release of heat at night. The cycle of heat absorption and release is necessary for a successful thermal storage wall. Figure 2.10 also shows that the fraction of PCM melted is greater in January than December. Although January is colder, the climate data in figure 2.8 shows January having almost twice the solar radiation of December. Therefore, the transmission of solar radiation isa more critical property of the glazing material than temperature insulation to successful passive solar heating.

Using the liquid fraction plot, the amount of heat stored and released to the air space during the five-day period can be calculated. Figure 2.11 shows a plot of the total heat stored and the total heat released for each day and container type in the five-day period modeled.

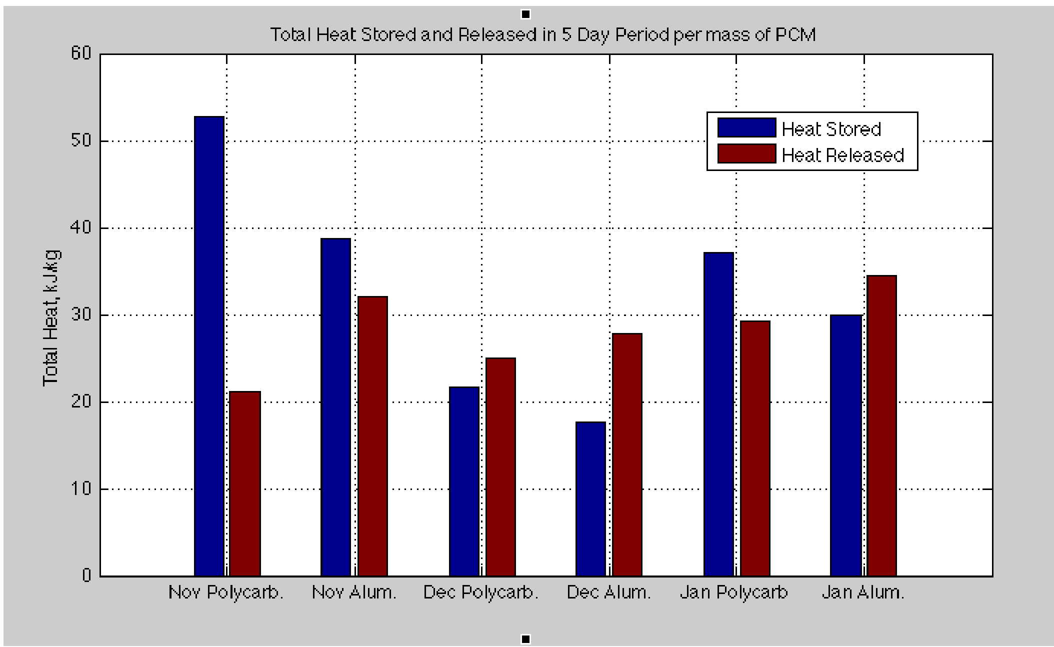

Figure 2.11: Total Heat stored and Released in a Five-day Simulation Period per mass of PCM

Figure 11 shows that the heat stored and released for both types of containers on all three representative winter days is significant. However, a well performing heat storage system will have roughly equal heat storage and release with time. If the system does not cycle effectively, heat is stored in the PCM but it it does not benefit the interior airspace. It could also melt completely and not re-solidify, again negating the positive aspects of latent heat storage. In November and January, the aluminum container was more effective at cycling the heat stored, while in December the polycarbonate was a more effective container material. It can also be noted that the PCM encapsulated in polycarbonate always stored more heat than the aluminum encapsulation, while the aluminum always released more heat. This trend indicates that with a polycarbonate container, the PCM would become completely melted over time and not exhibit the desired heat cycling characteristics. Although the results did not definitively indicate that aluminum or polycarbonate was a more effective container material, the insulating effects of polycarbonate suggest that aluminum is the better container material.

The temperature of the air space where the PCM heat was released was also studied. The air space temperature was taken to be an area-based average over the entire air space. Figure 2.12 shows the temperature of the air space with time for each scenario.

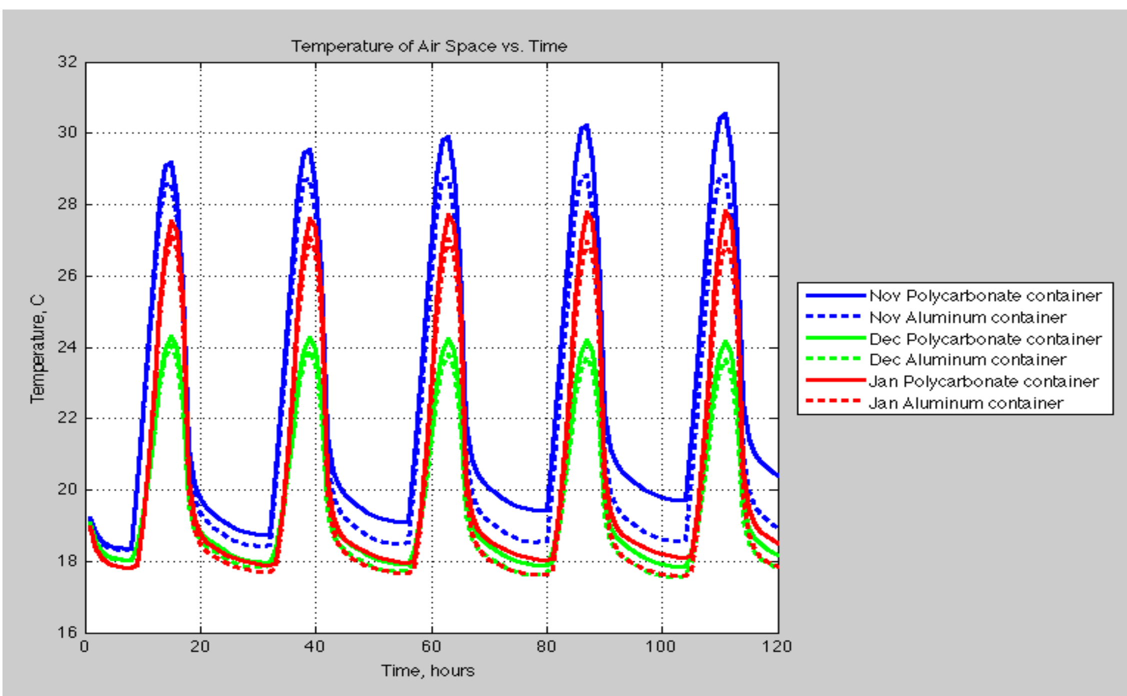

Figure 2.12: Temperature of the Air Space vs. Time

Figure 2.12 indicates that the temperature of the air gap with aluminum contained PCM is always lower than that of the polycarbonate contained PCM. It is important to compare the temperature of the air gap with that of the heat flux to the interior airspace of the house. Figure 2.13 provides an area-based average of heat flux through the interior wall.

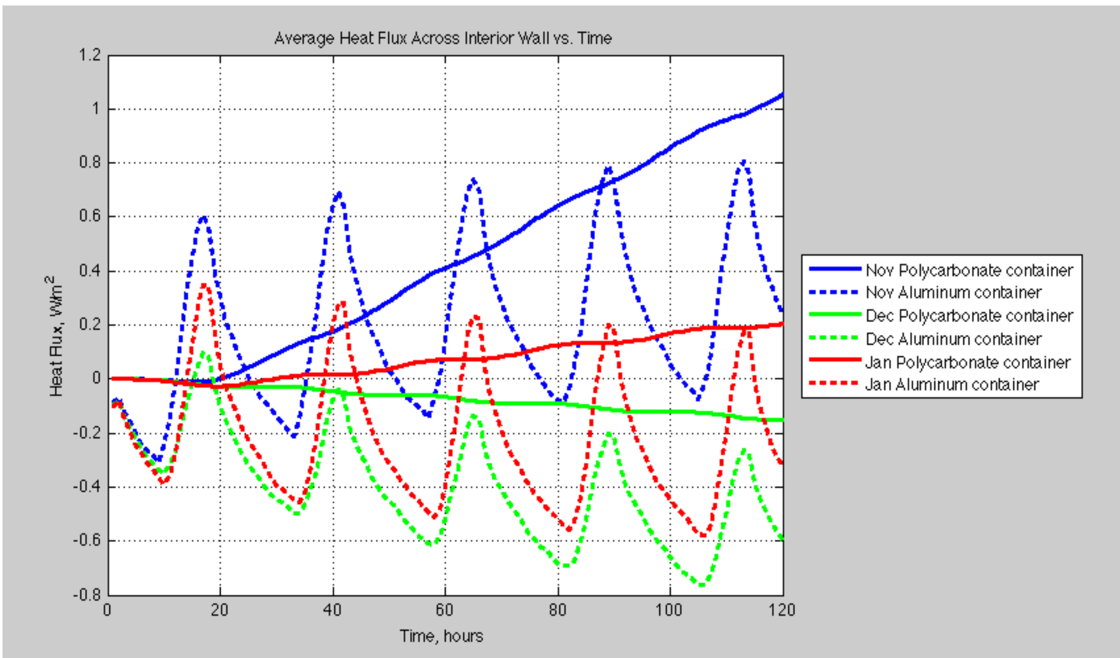

Figure 2.13: Average Heat Flux across the Interior Wall vs. Time

Figure 2.13 indicates that overall very little heat is being added or lost through the interior wall. Since the goal of the thermal storage wall is to add heat to the interior of the house, the lack of heat flux through the interior wall indicates that the current wall system is not properly designed. It is likely that the PCM is cycling heat to the wall air gap, rather than directly to the interior of the house. Furthermore, a comparison of Figure 2.12 and Figure 2.13 shows that there is a greater correlation between the airspace temperature and the aluminum container wall flux, than the polycarbonate contained PCM. In fact, the heat flux from the polycarbonate contained PCM is approximately linear over time. It is likely that the two figures do not directly correspond because the air gap temperature is an area average. While observing the simulation, it was obvious that both containers caused the heat to be focused on the exterior- or south-side of the air gap, where the solar radiation was being added. This also concentrated the melting of the PCM towards the south-side of the wall. As a result, most of the heat in the airspace was concentrated on the south side, and thus did not add heat to the interior of the house. In addition, the PCM melted on the south side of the container first, so the heat absorbed and released would be more focused to that side. Figure 2.14 shows an image of the temperature distribution at time hour 72 during the simulation of a polycarbonate container in December. In this picture, you can clearly see how the temperature is concentrated to the exterior side of the wall cavity.

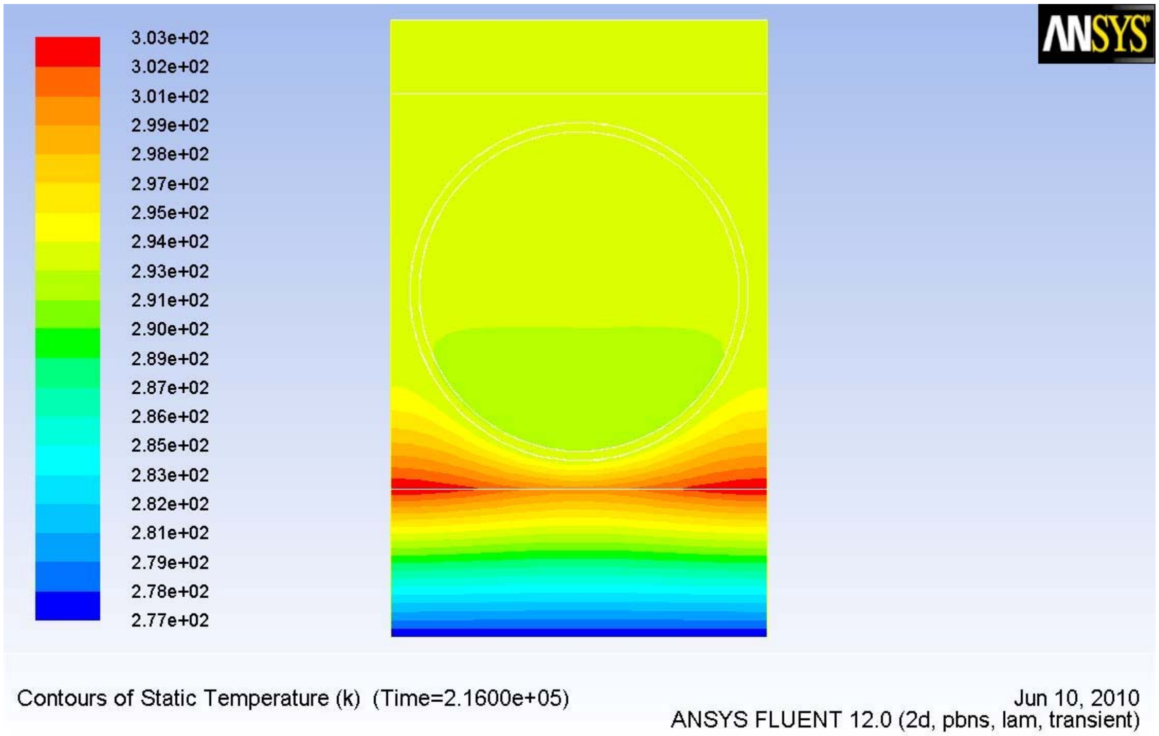

Figure 2.14: Temperature of Simulation at t=60 hours for Polycarbonate Container on December 15

Lastly, the performance of the PCM filled wall was compared to that of an empty wall. Figure 2.15 shows the heat flux across the interior wall for both PCM encapsulation materials as well as the empty wall section for each representative day. Figure 2.16 shows the area average air space temperature for the same conditions.

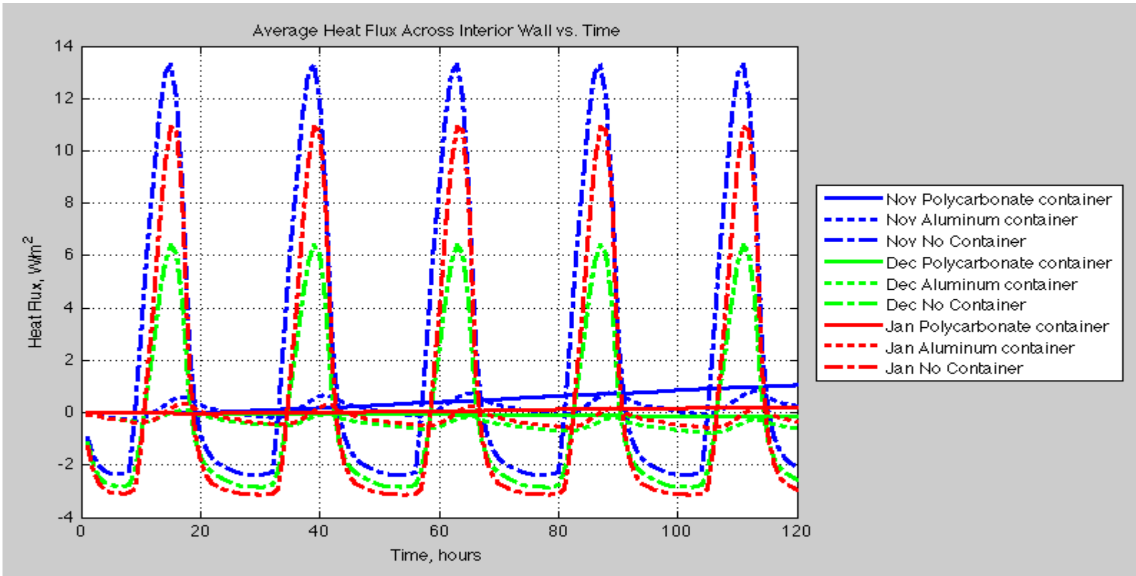

Figure 2.15: Average Heat Flux Across the Interior Wall vs. Time for PCM-filled and Empty Wall Sections

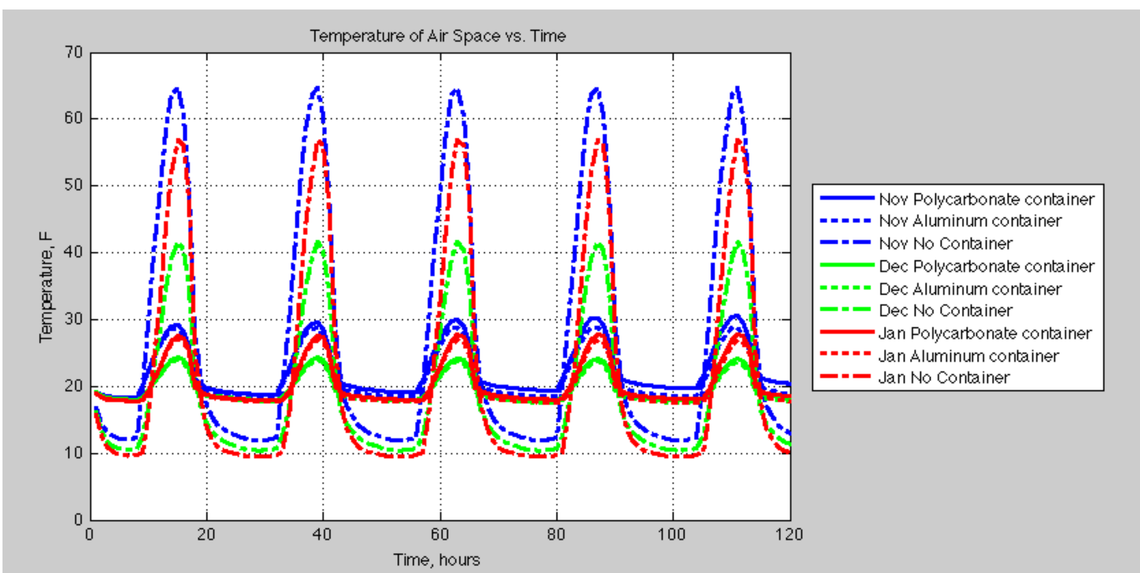

Figure 2.16: Average Air Space Temperature vs. Time for PCM-filled and Empty Wall Sections

Figures 2.15 and 2.16 both indicate that the PCM containers do an excellent job of moderating both the air gap temperature and the heat flux to the interior wall space.

Figure 2.15 shows the more heat is added and lost to the interior of the house with no PCM, which would be a benefit on sunny days, but a strong negative on cloudy days. This is similar to standard window performance.

4. Conclusions

The results generated by the FLUENT numerical model indicate that there is a significant quantity of heat absorbed and released from the PCM over time. However, this does not result in a direct benefit to the house interior airspace because the PCM is cycling heat in the storage wall air gap, not directly to the house interior. The resulting heat flux across the interior wall was very small, and not always in the positive direction. Furthermore, the results showed that the PCM wall performed worse on the moderate winter day than the severe one because there was less solar radiation. This underscores the importance of direct solar radiation to the performance of a PCM filled thermal storage wall. The two layers of Polygal used on the exterior severely limited the solar radiation to the PCM container, and thus the performance of the thermal storage wall. The numerical results did not conclusively show that aluminum was a better container material then polycarbonate, although it was significantly better at cycling the heat absorbed and released. This would suggest that aluminum is the better encapsulation material, but further investigation would be required to prove this conclusion. However, the numerical analysis definitively showed that the PCM containers moderated both the wall air gap temperature and the heat flux through the wall, which would be a significant benefit in colder climates with many cloudy days.

The conclusions drawn from the numerical analysis also gives clues on how the 2009 Solar Decathlon house thermal storage wall could be significantly improved for better passive solar heating. Replacing the Polygal with a high-performance glass would significantly increase the solar heat gain to the PCM material and improve the overall system performance. Another suggested change is to make the interior wall the thermal storage element. Then, the PCM would cycle heat to and from the interior air space rather than to the air gap in the wall. The benefits of the PCM would affect the interior directly, rather than secondarily through heat transfer to the air gap and then to the house interior. This would involve changing the macro-encapsulation scheme but would result in a more effective system.

Further investigation of the effects of thermal conductivity between the PCM and its surroundings is suggested for future research. This would involve a study of the performance of the encapsulated PCM for representative months or seasons, rather than days. Conductive materials other than aluminum could be evaluated. The addition of a metal matrix to the PCM could also be investigated as a way to improve the uniformity of melting within the material and heat transfer to the surroundings. Along with making the interior wall the thermal storage element, other shapes and sizes for containers could be evaluated. Results of these studies would significantly aid the design of a thermal storage wall incorporating macro-encapsulated PCM for passive solar heating.

5. References

[1] 2009, "Annual Energy Review 2008", Energy Information Administration, United States Government Printing Office, p. 3, http://www.eia.doe.gov/emeu/aer/pdf/pages/sec1.pdf.

[2] 2008, "2005 Residential Energy Consumption Survey: Household Consumption and Expenditures Tables", Energy Information Administration, United States Government Printing Office, p.1, http://www.eia.doe.gov/emeu/recs/recs2005/c&e/summary/pdf/tableus12.pdf.

[3] Lane, G.A.,1983, *Solar Heat Storage: Latent Heat Materials*, CRC Press, Inc., Boca Raton, FL, Vol. 1.

[4] 2007 ASHRAE Handbook – Heating, Ventilating, and Air-Conditioning Applications (I-P Edition), American Society of Heating, Refrigeration and Air-Conditioning Engineers, Inc, chapter 34.1.

[5] Mehling, H. & Cabeza, L.F., 2008, *Heat and Cold Storage with PCM*, Springer, Berlin.

[6] Telkes, M., 1978, "Trombe Wall with Phase Change Storage Material", *Proceedings of the 2nd National Passive Solar Conference*, Philadelphia, PA.

[7] Lou, D.Y.S, 1983, "Solidification Process in Glauber Salt Mixture", *Solar Energy*, 30(2), pp. 115-121.

[8] Marks, S.B., 1983, "The Effect of Crystal Size on the Thermal Energy Storage Capacity of Thickened Glauber's Salt", *Solar Energy*, 30(1), pp. 45-49.

[9] Onwubiko, C. & Russell, L.D., 1984, "Experimental Investigation of Physical Characteristics of Glauber's Salt as a Storage Medium", *Solar Energy*, 33(5), pp. 465-467.

[10] Lane G.A., 1986, *Solar Heat Storage: Latent Heat Materials*, CRC Press, Inc., Boca Raton, FL, Vol 2.

[11] Khudhair, A.M. & Farid, M.M., 2004, "A Review on Energy Conservation in Building Applications with Thermal Energy Storage by Latent Heat Using Phase Change Materials", *Energy Conversion and Management*, 45, pp. 263-275.

[12] Zhang, Y., Zhou, G., Lin, K., Zhang, Q. & Di, H., 2007, "Application of Latent Heat Thermal Energy Storage: State-of-the-art and Outlook", *Building and Environment*, 42, pp. 2197-2209.

[13] Sharma, S.D. & Sagara, K., 2005, "Latent Heat Storage Materials and Systems: A Review", *International Journal of Green Energy*, 2, pp. 1-56.

[14] Pieppo, K., Kauranen, P., & Lund, P.D., 1991, "A Multicomponent PCM Wall Optimized for Passive Solar Heating", *Energy and Buildings*, 17, pp. 259-270.

[15] Scalat, S., Banu, D., Hawes, D., Paris, J., Haghighata, F., & Feldman, D., 1996, "Full Scale Thermal Testing of Latent Heat Storage in Wallboard", *Solar Energy Materials and Solar Cells*, 44, pp. 49-61.

[16] Neeper, D.A., 2000, "Thermal Dynamics of Wallboard with Latent Heat Storage", *Solar Energy*, 68(5), pp. 393-403.

[17] Voelker, C., Kornadt, O., & Ostry, M., 2008, "Temperature Reduction due to the Application of Phase Change Materials", *Energy and Buildings*, 40, pp. 937-944.

[18] Castellón, C., Castell, A. Medrano, M. Martorell, I., & Cabeza, L.F., 2009, "Experimental Study of PCM Inclusion in Different Building Envelopes", *Journal of Solar Energy Engineering*, 131, pp. ***NEED PAGE NUMBERS

[19] Knowles, T.R., 1983, "Proportioning Composites for Efficient Thermal Storage Walls", *Solar Energy*, 31(3), pp. 319-326.

[20] Benard, C., Body, Y., & Zanoli, A., 1985, "Experimental Comparison of Latent Heat and Sensible Heat Thermal Walls", *Solar Energy*, 34(6), pp. 475-487.

[21] Carbonari, A., De Grassi, M., Di Perna, C., & Principi, P., 2006, "Numerical and Experimental Analysis of PCM Containing Sandwich Panels for Pre-fabricated Walls", *Energy and Buildings*, 38, pp. 472-483.

[22] Ahmad, M., Bontemps, A., Sallée, H., & Quenard, D., 2006, "Experimental Investigation and Computer Simulation of Thermal Behaviour of Wallboards Containing a Phase Change Material", *Energy and Buildings*, 38, pp. 357-366.

[23] Lebens, Ralph M., 1980, *Passive Solar Heating Design*, Applied Science Publishers Ltd, London, UK.

[24] Steven Winter Associates, Inc., 1983, *The Passive Solar Construction Handbook*, Rodale Press, Emmaus, PA.

[25] 2007, "Polyethylene Glycol 600," MSDS No. UCN0038E (2007), Univar USA Inc, Redmond, WA.

[26] 2010, “Thermogal 25-40mm Technical Specifications”, Polygal, http://www.polygal.com/index.php?option=com_content&view=article&id=112&Itemid=106

[27] Voller, V.R. & Prakash, C., 1987, “A Fixed Grid Numerical Modeling Methodology for Convection-diffusion Mushy Region Phase-change Problems”, *International Journal of Heat and Mass Transfer*, 30(8), pp. 1709-1719.

[28] 2006, “Chapter 24. Modeling Solidification and Melting”, *FLUENT 6.3 User’s Guide*, Fluent Inc, Lebanon, NH, pp. 24-1 – 24-4.

[29] 2009 ASHRAE Handbook - Fundamentals (I-P Edition), American Society of Heating, Refrigerating and Air-Conditioning Engineers, Inc, pp.17.1-17.16.

[30] “National Solar Radiation Database: 1991-2005 Update”, Renewable Resource Database, National Renewable Energy Lab, http://rredc.nrel.gov/solar/old_data/nsrdb/1991-2005/hourly/siteonthefly.cgi?id=724280

[31] “History for Columbus, OH”, Weather Underground, http://www.wunderground.com/history/airport/KCMH/

[32] Ismail, K.A.R., Henriquez, J.R., & Salinas, C.T., 2008, “Comparison Between PCM Filled Glass Windows and Absorbing Gas Filled Windows”, *Energy and Buildings,* 40, pp. 710-719.

References

2009, “Annual Energy Review 2008”, Energy Information Administration, United States Government Printing Office, p. 3, http://www.eia.doe.gov/emeu/aer/contents.html.

Marion, W. & Wilcox, S., 1994, “Solar Radiation Data Manual for Flat-Plate and Concentrating Collectors”, National Renewable Energy Lab, p. 3, http://rredc.nrel.gov/solar/pubs/redbook/.

1994, “30 Year Average of Monthly Solar Radiation, 1961-1990”, National Renewable Energy Lab Renewable Resource Data Center, http://rredc.nrel.gov/solar/old_data/nsrdb/redbook/sum2/state.html

2008, “PV Watts Version 1 Calculator,” National Renewable Energy Lab Renewable Resource Data Center, http://rredc.nrel.gov/solar/calculators/PVWATTS/version1/

2009, “Average Retail Price of Electricity to Ultimate Customers: Total by End-Use Sector”, Electric Power Monthly, No. DOE/EIA-0226 (2009/12), Energy Information Administration, p. 104, http://www.eia.doe.gov/cneaf/electricity/epm/epm.pdf

Lutz, J. D., Liu, X., McMahon, J. E., Dunham, C., & McGrue, Q. T., 1996, "Modeling Residential Hot Water Use Patterns," No. LBL-37805, Lawrence Berkeley National Laboratory.

“SOLARHOT Platinum Series,” SolarHOt, Morrisville, NC, http://www.solarhotusa.com/support/literature/files/collector.pdf

Energy Information Administration, 2009, “Annual Ohio Price of Natural Gas Delivered to Residential Consumers,” http://tonto.eia.doe.gov/dnav/ng/hist/n3010oh3a.htm.

Christian, J., Desjarlais, A., & Kosny, J., 1999. “Whole Wall Rating/Label for Structural Insulated Panels: Steady-State Thermal Analysis,” Oak Ridge National Laboratory Buildings Technology Center, http://www.sips.org/elements/uploads/files/fileManager/WholeWallR-ValueStudy.pdf

Arif, M. & Mullens, M.A., 2006, “Structural Insulated Panels: Impact on the Residential Construction Process,” Journal of Construction Engineering and Management, 132(7) pp. 786-795.

2005, “The Facts About Solar Heat Gain & Windows,” National Fenestration Rating Council, http://www.nfrc.org/documents/U-Factor.pdf

2005, “The Facts About Windows & Heat Loss,” National Fenestration Rating Council, http://www.nfrc.org/documents/U-Factor.pdf

2007 ASHRAE Handbook - Heating, Ventilating, and Air-Conditioning Applications (I-P Edition), American Society of Heating, Refrigerating and Air-Conditioning Engineers, Inc, pp. 34.1-34.2.

Sharma, S.D. & Sagara, K., 2005, “Latent Heat Storage Materials and Systems: A Review,” International Journal of Green Energy, 2, pp. 1-56.

Zhang, Y., Zhou, G. , Lin, K., Zhang, Q., & Di, H., 2006, “Application of Latent Heat Thermal Energy Storage in Buildings: State-of-the-Art and Outlook,” Building and Environment, 42, pp. 2197-2209.

2007, “Polyethylene Glycol 600,” MSDS No. UCN0038E (2007), Univar USA Inc, Redmond, WA.

2006, “CARBOWAX Polyethylene Glycols and Methoxypolyethylene glycols,” Dow Chemical Company: Midland, MI, http://www.dow.com/polyglycols/carbowax/resource/index.htm

2009 ASHRAE Handbook - Fundamentals (I-P Edition), American Society of Heating, Refrigerating and Air-Conditioning Engineers, Inc, pp.17.1-17.16.

Watson, R.D. & Chapman, K. S., 2002, Radiant Heating and Cooling Handbook, McGraw-Hill, New York, NY, pp. 4.1-4.8.

2006, “The Department of Natural Resources Division of Water Fact Sheet: Efficiency at Home,” Ohio Department of Natural Resources Division of Water, Columbus, Ohio, http://www.dnr.state.oh.us/Portals/7/pubs/pdfs/fctsht01.pdf

Rozgus, A., 2009, “Using Gray Water Efficiently,” Consulting-Specifying Engineer, 45(3), p. 19-20.

2008, “AQUS System Specifications,” WaterSaver Technologies, Louisville, KY, http://www.watersavertech.com/AQUS_Specifications_Sheet.pdf

2009, “Annual Energy Review 2008”, Energy Information Administration, United States Government Printing Office, p. 3, http://www.eia.doe.gov/emeu/aer/pdf/pages/sec1.pdf.

2008, “2005 Residential Energy Consumption Survey: Household Consumption and Expenditures Tables”, Energy Information Administration, United States Government Printing Office, p.1, http://www.eia.doe.gov/emeu/recs/recs2005/c&e/summary/pdf/tableus12.pdf.

Lane, G.A.,1983, *Solar Heat Storage: Latent Heat Materials*, CRC Press, Inc., Boca Raton, FL, Vol. 1.

2007 ASHRAE Handbook – Heating, Ventilating, and Air-Conditioning Applications (I-P Edition), American Society of Heating, Refrigeration and Air-Conditioning Engineers, Inc, chapter 34.1.

Mehling, H. & Cabeza, L.F., 2008, *Heat and Cold Storage with PCM*, Springer, Berlin.

Telkes, M., 1978, "Trombe Wall with Phase Change Storage Material", *Proceedings of the 2nd National Passive Solar Conference*, Philadelphia, PA.

Lou, D.Y.S, 1983, "Solidification Process in Glauber Salt Mixture", *Solar Energy*, 30(2), pp. 115-121.

Marks, S.B., 1983, "The Effect of Crystal Size on the Thermal Energy Storage Capacity of Thickened Glauber's Salt", *Solar Energy*, 30(1), pp. 45-49.

Onwubiko, C. & Russell, L.D., 1984, "Experimental Investigation of Physical Characteristics of Glauber's Salt as a Storage Medium", *Solar Energy*, 33(5), pp. 465-467.

Lane G.A., 1986, *Solar Heat Storage: Latent Heat Materials*, CRC Press, Inc., Boca Raton, FL, Vol 2.

Khudhair, A.M. & Farid, M.M., 2004, "A Review on Energy Conservation in Building Applications with Thermal Energy Storage by Latent Heat Using Phase Change Materials", *Energy Conversion and Management*, 45, pp. 263-275.

Zhang, Y., Zhou, G., Lin, K., Zhang, Q. & Di, H., 2007, "Application of Latent Heat Thermal Energy Storage: State-of-the-art and Outlook", *Building and Environment*, 42, pp. 2197-2209.

Sharma, S.D. & Sagara, K., 2005, "Latent Heat Storage Materials and Systems: A Review", *International Journal of Green Energy*, 2, pp. 1-56.

Pieppo, K., Kauranen, P., & Lund, P.D., 1991, "A Multicomponent PCM Wall Optimized for Passive Solar Heating", *Energy and Buildings*, 17, pp. 259-270.

Scalat, S., Banu, D., Hawes, D., Paris, J., Haghighata, F., & Feldman, D., 1996, "Full Scale Thermal Testing of Latent Heat Storage in Wallboard", *Solar Energy Materials and Solar Cells*, 44, pp. 49-61.

Neeper, D.A., 2000, "Thermal Dynamics of Wallboard with Latent Heat Storage", *Solar Energy*, 68(5), pp. 393-403.

Voelker, C., Kornadt, O., & Ostry, M., 2008, "Temperature Reduction due to the Application of Phase Change Materials", *Energy and Buildings*, 40, pp. 937-944.

Castellón, C., Castell, A. Medrano, M. Martorell, I., & Cabeza, L.F., 2009, "Experimental Study of PCM Inclusion in Different Building Envelopes", *Journal of Solar Energy Engineering*, 131, pp. ***NEED PAGE NUMBERS

Knowles, T.R., 1983, "Proportioning Composites for Efficient Thermal Storage Walls", *Solar Energy*, 31(3), pp. 319-326.

Benard, C., Body, Y., & Zanoli, A., 1985, "Experimental Comparison of Latent Heat and Sensible Heat Thermal Walls", *Solar Energy*, 34(6), pp. 475-487.

Carbonari, A., De Grassi, M., Di Perna, C., & Principi, P., 2006, "Numerical and Experimental Analysis of PCM Containing Sandwich Panels for Pre-fabricated Walls", *Energy and Buildings*, 38, pp. 472-483.

Ahmad, M., Bontemps, A., Sallée, H., & Quenard, D., 2006, "Experimental Investigation and Computer Simulation of Thermal Behaviour of Wallboards Containing a Phase Change Material", *Energy and Buildings*, 38, pp. 357-366.

Lebens, Ralph M., 1980, *Passive Solar Heating Design*, Applied Science Publishers Ltd, London, UK.

Steven Winter Associates, Inc., 1983, *The Passive Solar Construction Handbook*, Rodale Press, Emmaus, PA.

2007, "Polyethylene Glycol 600," MSDS No. UCN0038E (2007), Univar USA Inc, Redmond, WA.

2010, "Thermogal 25-40mm Technical Specifications", Polygal, http://www.polygal.com/index.php?option=com_content&view=article&id=112&Itemid=106

Voller, V.R. & Prakash, C., 1987, "A Fixed Grid Numerical Modeling Methodology for Convection-diffusion Mushy Region Phase-change Problems", *International Journal of Heat and Mass Transfer*, 30(8), pp. 1709-1719.

2006, "Chapter 24. Modeling Solidification and Melting", *FLUENT 6.3 User's Guide*, Fluent Inc, Lebanon, NH, pp. 24-1 – 24-4.

2009 ASHRAE Handbook - Fundamentals (I-P Edition), American Society of Heating, Refrigerating and Air-Conditioning Engineers, Inc, pp.17.1-17.16.

"National Solar Radiation Database: 1991-2005 Update", Renewable Resource Database, National Renewable Energy Lab, http://rredc.nrel.gov/solar/old_data/nsrdb/1991-2005/hourly/siteonthefly.cgi?id=724280

“History for Columbus, OH”, Weather Underground, http://www.wunderground.com/history/airport/KCMH/

Ismail, K.A.R., Henriquez, J.R., & Salinas, C.T., 2008, “Comparison Between PCM Filled Glass Windows and Absorbing Gas Filled Windows”, *Energy and Buildings,* 40, pp. 710-719.